



# Genetically encoded iron-associated proteins as MRI reporters for molecular and cellular imaging

Anna V. Naumova<sup>1,2\*</sup> and Greetje Vande Velde<sup>3</sup>

All cell imaging applications rely on some form of specific cell labeling to achieve visualization of cells contributing to disease or cell therapy. The purpose of this review article is to summarize the published data on genetically encoded iron-based imaging reporters. The article overviews regulation of iron homeostasis as well as genetically encoded iron-associated molecular probes and their applications for noninvasive magnetic resonance imaging (MRI) of transplanted cells. Longitudinal repetitive MRI of therapeutic cells is extremely important for providing key functional endpoints and insight into mechanisms of action. Future directions in molecular imaging and techniques for improving sensitivity, specificity and safety of *in vivo* reporter gene imaging are discussed. © 2017 Wiley Periodicals, Inc.

How to cite this article:

*WIREs Nanomed Nanobiotechnol* 2018, 10:e1482. doi: 10.1002/wnan.1482

## INTRODUCTION

Regeneration of injured organs by transplantation of specific cell populations is an area of intense interest in translational medicine. Since the pioneering work of Dr. E. D. Thomas in bone-marrow transplantation in the late 1950s,<sup>1</sup> along with Dr. J. E. Murray who pioneered kidney transplantation,<sup>2</sup> a large number of clinical studies have been conducted using different cell types. Drs. Thomas and Murray received a Nobel Prize in physiology and medicine in 1990 for their achievements. Clinical studies have since demonstrated the safety and feasibility of transplanting adult stem cell derivatives (i.e., bone-marrow cells, mesenchymal stem cells, skeletal

myoblasts, and cardiac/endothelial progenitor cells, adipose tissue-derived cells), but unfortunately, long-term benefits have been modest.<sup>3,4</sup> Considerable progress has been made in recent years in the development of new sources of transplantable cells [e.g., derivatives of human embryonic stem cells (ESCs) and induced pluripotent stem cells (iPSCs)] and manipulation of endogenous stem cell pools<sup>5</sup> in applications to repair-specific organs, such as heart,<sup>6,7</sup> brain,<sup>8–10</sup> spinal cord,<sup>11,12</sup> retina,<sup>13–16</sup> liver,<sup>17</sup> and pancreas.<sup>18</sup> Despite considerable breakthrough in cell transplantation, many questions remain unanswered regarding survival and migration of the transplanted cells to an injury site, their engraftment and functional integration within host tissues, immunogenicity and tumorigenicity, etc. *Ex vivo* histological or immunohistochemical staining methods provide the most detailed picture of the transplant on cellular and tissue level with high spatial resolution, but they lack individual dynamic information and require the sacrifice of large numbers of animals in order to complete longitudinal studies. *In vivo* molecular imaging technology might serve as a valuable tool for guiding cell therapy by visualization of biological processes on the cellular

\*Correspondence to: nav@uw.edu

<sup>1</sup>Department of Radiology, University of Washington, Seattle, WA, USA

<sup>2</sup>Research Institute of Biology and Biophysics, National Research Tomsk State University, Tomsk, Russia

<sup>3</sup>Department of Imaging and Pathology, KU Leuven - University of Leuven, Leuven, Belgium

Conflict of interest: The authors have declared no conflicts of interest for this article.

and subcellular levels, enabling the longitudinal, non-invasive monitoring of the *in vivo* fate and function of transplanted cells.<sup>19</sup>

Various imaging modalities such as radionuclide, optical, magnetic resonance imaging (MRI), computed tomographic, and ultrasound can be used for anatomic and functional assessment of organs after cell therapy and for *in vivo* cell tracking. Specific research questions determine the choice of imaging modality. Several constructive reviews have been published in recent years outlining the uses of each imaging modality for cell tracking, achievable image resolution, and scan time.<sup>20–25</sup> Superior soft-tissue contrast, large availability of imaging techniques, variety of contrast mechanisms, multinuclear capability, absence of ionizing radiation (safety), as well as capability for monitoring functional, anatomical and metabolic information enable MRI to stand out. MRI contrast weighting techniques can detect areas of pathology (scar, inflammation),<sup>26</sup> volume loss,<sup>27</sup> complex tissue architecture,<sup>28,29</sup> chemical exchange within the macromolecular environment,<sup>30,31</sup> cellular death and inflammation,<sup>32–34</sup> metabolite concentration,<sup>35–37</sup> tissue perfusion,<sup>38–40</sup> and vascularity.<sup>41–43</sup> Recent advances in MRI reporter gene techniques have enabled *in vivo* imaging of specific cell populations of interest regarding cell survival, proliferation, migration, and differentiation,<sup>24,44–50</sup> which makes MRI a valuable technology among other molecular imaging modalities.

In molecular and cellular imaging, imaging probes are required to label cells or to target the biological processes of interest. The imaging probe usually consists of a carrier (such as nanoparticle, microbubble, liposome, etc.) and a signal element or contrast agent that is recognized by the corresponding imaging system. An imaging probe may or may not contain a targeting element so that the contrast agents either bind to specific cell surface proteins or are transported into the target cell by diffusion, endocytosis, or active transport (e.g., radiolabeled indium oxine and superparamagnetic iron oxide particles).<sup>20,23,24</sup> Another way to label cells is integration of reporter genes into cellular DNA. Transgene then will be transcribed into messenger RNA and translated into proteins that are detectable by an imaging modality or interact with a molecular probe for imaging signal generation, for example ferritin<sup>51–54</sup> and transferrin,<sup>55–57</sup> bivalent metal transporters DMT1<sup>58</sup> and Timd2,<sup>59–61</sup> CEST reporters,<sup>32,33</sup> expressible reporters based on gas vesicles,<sup>62</sup> etc.

Cell labeling by using a contrast agent carrier system (e.g., iron oxide nanoparticles) is relatively

easy to accomplish; this labeling technique provides the strong signal on <sup>1</sup>H MRI that allows high-resolution visualization of the migration and homing of injected cells. However, this approach has several drawbacks for long-term imaging, because the imaging probe is diluted as cells divide, which results in a gradual disappearance of the contrast.<sup>63–65</sup> Moreover, nanoparticle-based imaging cannot distinguish live and dead cells<sup>66–68</sup> and high doses of iron-oxide nanoparticles used in MRI raise concerns of cellular toxicity.<sup>69,70</sup> Therefore, carrier imaging systems (such as iron nanoparticles) are best suited for non-invasive determination of transplanted cell localization and are not useful for longer-term monitoring of engraftment and survival. A transgene expression approach allows overcoming these disadvantages. With the right choice of gene-delivery method, reporter genes can incorporate stably into the DNA and will propagate to daughter cells. In this case, the resulting imaging signal reflects transplanted cell viability and quantity. Reporter gene expression is a better marker for monitoring cell viability, therefore this labeling concept is more suitable for assessing long-term grafted cell survival<sup>68,71</sup> (Figure 1).

The purpose of this review article is to summarize the published data on genetically encoded iron-associated reporters, to discuss their advantages and weaknesses. First, we provide overview of iron homeostasis regulation and genetically encoded iron-associated molecular probes used for noninvasive MRI of transplanted cells. Then we discuss the most important applications of iron-associated MR reporters in studies of cell transplantation in brain, heart, and tumors. In conclusion, we discuss the future directions in molecular imaging and techniques for improving sensitivity of *in vivo* MR reporter imaging and transition into the clinical trials.

## IRON AND MRI CONTRAST

### Effect of Iron on MRI Contrast

MRI contrast is dependent on tissue relaxation properties in a magnetic field following a radio frequency (RF) excitation pulse. The spin–lattice ( $T_1$ ) relaxation time characterizes the return of nuclear spins to the equilibrium state along the direction of the static magnetic field ( $B_0$ ). The spin–spin ( $T_2$ ) relaxation time characterizes the loss of spin coherence and net magnetization in the transverse plane. A relaxation mechanism of coherent transverse magnetization, called  $T_2^*$  decay, combines effects of  $B_0$ -inhomogeneities, susceptibility artifacts, and

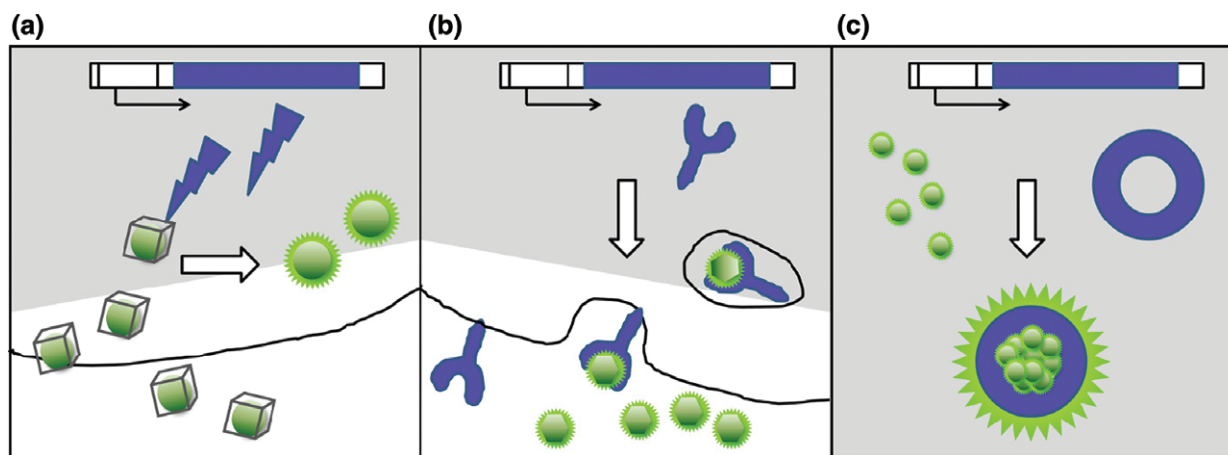


**FIGURE 1** | Mechanisms for cell labeling through (semi-) genetic control of MR imaging contrast. *LacZ* is the gene that encodes  $\beta$ -galactosidase.<sup>72</sup> Tfr: transferrin receptor. (a) A genetically expressed enzyme (blue) alters an exogenously administered imaging probe (green) that becomes active (green halo) upon enzyme processing (e.g., *lacZ*). (b) Gene expression leads to the synthesis of a cell surface protein (blue) that acts as a receptor for an exogenous contrast agent (green) and subsequently promotes agent internalization (e.g., Tfr). (c) A gene directs endogenous production of protein (blue) that becomes a MRI contrast agent in complex with endogenous ions (green) (e.g., ferritin, magA).

chemical shifts that affect MRI contrast generation. Positive (bright) contrast is typically generated with contrast agents shortening  $T_1$  relaxation, such as gadolinium ( $Gd^{3+}$ ) or manganese ( $Mn^{2+}$ ). Iron accumulation in cells and tissues affects the transverse ( $T_2$ ) magnetic relaxation and  $T_2^*$ -weighted MR images based on magnetic susceptibility effects. It creates dark areas of signal hypointensity, also referred to as negative contrast.

Superparamagnetic iron-oxide (SPIO) nanoparticles are the most popular agents for cell labeling. Cells may be easily directly labeled with SPIOs by adding these nanoparticles to cell media with or without transfection reagents. High intracellular concentrations of the SPIOs provide strong image contrast as signal void areas on  $T_2^*$ -weighted images (decrease in signal intensity in areas of particle accumulation up to 80–90%<sup>68</sup>) or as areas of reduced  $T_2$ -relaxation on calculated  $T_2$ -maps.<sup>68,73–75</sup> SPIO-tagged cells can also be directly imaged by magnetic particle imaging.<sup>76,77</sup> This recently introduced technique directly detects the intense magnetization of synthetic iron-oxide tracers using low-frequency magnetic fields which enables monitoring of cellular grafts with high contrast, sensitivity, and provides highly quantitative ‘hot spot’ imaging.<sup>78,79</sup>

MRI contrast can also be enhanced by manipulation of the iron content in cells through the utilization of iron-associated proteins as contrast agents. Iron-associated gene reporters exhibit smaller changes in MRI contrast and transverse relaxation in  $T_2$ - and  $T_2^*$ -weighted sequences in comparison with

iron oxide nanoparticles: the observed decrease in signal intensity is in the range of 20–30 % in lower magnetic field strengths<sup>68,80</sup> and up to 50% at higher field strengths.<sup>80–82</sup> Weaker MRI contrast properties of iron-associated reporters are determined by the structure of the ferrihydrite mineral core, that contains fewer iron atoms<sup>83</sup> as well as alignment of the iron magnetic spin moments causing smaller net magnetization.<sup>84,85</sup> Not only the reporter transgene itself, but also the right choice of gene expression system is essential for optimal MRI contrast generation in the target cell population (Box 1).

### Iron Homeostasis

Iron is one of the essential elements for life because of its ability to donate and accept electrons with relative ease. Many proteins and enzymes have iron as an integral cofactor critical for numerous biological functions, such as oxygen binding and transport (hemoglobins), oxygen metabolism (catalases, peroxidases), cellular respiration, electron transport (cytochromes), and fundamental cellular processes such as DNA synthesis, cell proliferation and differentiation (ribonucleotide reductase), gene regulation, drug metabolism, and steroid synthesis.<sup>86</sup> Iron deficiencies as well as iron overload lead to diverse pathological changes. Iron deficiency results from defects in acquisition or distribution of the metal and causes anemia. In opposite, high concentrations of iron are toxic for cells, because free iron catalyzes radical formation in oxygenated tissues (Fenton’s reaction) leading to cell

## BOX 1

## REPORTER GENE EXPRESSION SYSTEMS

A plethora of options exist for transgene expression of a mammalian target cell population. Over the past few decades, different types of gene expression systems and delivery vectors have been engineered for genetic editing of mammalian cells, based on mixing and matching genes, promoters, and regulatory sequences found in nature. Not only for assembling the expression cassette and genome editing do there exist different elements and methods, also for delivery are there different viral and nonviral vehicles at hand, that are extensively reviewed elsewhere.<sup>164–169</sup> The characteristics of each technique for genetic labeling of cells will determine a great deal of the properties of contrast generation; whether this will be inducible, transient or stable, cell-type or tissue-specific, as well as transgene expression level. Therefore, not only the reporter transgene itself, but also the right choice of gene expression system is essential for optimal MRI contrast generation in the target cell population.

damage. Iron homeostasis is therefore tightly regulated in the organism for maintaining the balance between iron storage and utilization by controlling intestinal absorption of the metal from the diet along with the expression of iron transport and storage proteins such as transferrin, transferrin receptor (TfR), hepcidin, and ferritin.

The human body contains approximately 3–5 g of iron present as heme in hemoglobin of erythrocytes (>2 g), myoglobin of muscles (~0.3 g), in macrophages of spleen, liver, and bone marrow (~0.6 g). Excess of the metal is stored in the liver parenchyma within ferritin (~1 g).<sup>87</sup> All other cellular iron containing proteins and enzymes bind an estimated total of approximately 0.008 g of iron. Iron is delivered to erythroblasts and to most tissues via circulating *transferrin*, which carries approximately 0.003 g of the metal at steady-state. In humans, plasma transferrin is normally about 30% saturated with iron. A transferrin saturation of 45% is a sign of iron overload. When the saturation exceeds 60%, non-transferrin-bound iron begins to accumulate in the circulation and to damage parenchymal cells.<sup>88</sup>

Most mammalian cells acquire iron from circulating transferrin upon binding of the transferrin-iron

complex to the TfR. The TfR is a homodimer transmembrane glycoprotein with an overall molecular weight of approximately 180 kDa, located at the cell surface. It is ubiquitously expressed in almost all cells,<sup>89</sup> with higher levels of expression in highly proliferating cells and those that have a functional need for iron.<sup>86</sup> TfRs are therefore naturally present in large numbers in erythrocyte precursors, placenta, and liver.<sup>90–93</sup> The main function of transferrin is mediation of iron internalization through receptor-mediated endocytosis. Most eukaryotic cells use receptor-mediated endocytosis almost exclusively for Fe(III)-TfR uptake.<sup>94</sup> Iron is released from the TfR complex by a pH-change in the endosomal compartment, caused by proton-pump ATPase-activity.<sup>95</sup> The TfR tightly controls cellular iron homeostasis by regulating cellular uptake of holo-transferrin.<sup>96</sup> Mutations in the transferrin gene cause severe anemia.<sup>88</sup> Targeted deletion of the mouse transferrin gene causes embryonic lethality at day E11.5 due to severe anemia, indicating that transferrin-mediated iron delivery is indeed critical for hematopoietic cells.<sup>97</sup>

Cytosolic iron is transported to intracellular sites either for local use or for storage in *ferritin*. Ferritin is found in most cell types of humans, animals, vertebrates, invertebrates, higher plants, fungi, and bacteria, but the concentration of the protein among different cell types can vary 1000-fold. The iron storage protein ferritin consists of a spherical polypeptide shell (apoferritin) surrounding a 6-nanometer inorganic core of the hydrated iron oxide ferrihydrite [Fe<sub>5</sub>O<sub>3</sub>(OH)]<sub>9</sub>.<sup>98</sup> The mammalian apoferritin is a hollow sphere composed of 24 heavy (H; 21 kDa) and light (L; 19 kDa) folded chains. The apoferritin shell can accommodate up to 4500 iron atoms attached to the inner wall of the shell.<sup>99–101</sup> More recent data suggest as few as 1100 iron atoms in ferritin.<sup>102</sup> Iron load in ferritin is dependent of the H<sub>2</sub>O<sub>2</sub> detoxification reaction and can be at low, intermediate, and high iron level.<sup>103,104</sup>

Ferritin stores iron in soluble form, available for use by enzymes and for DNA synthesis. Both ferritin subunits are ubiquitously expressed, but their expression ratios vary depending on the cell type and in response to stimuli such as inflammation or infection. Ferritin H-chain has the ferroxidase activity that is necessary for iron deposition into the nanocage, while ferritin L-chain facilitates iron nucleation and increases the turnover of the ferroxidase site. Ferritin provides cells with a means to lock up excess iron in a redox-inactive form to prevent iron-mediated cell and tissue damage.<sup>105–107</sup>

There are three variations in ferritin function in different cell types: (1) the storage of iron for other cells (e.g., recycling iron in macrophages, short- and long-term iron storage in red blood cells of embryos or in hepatocytes of adults); (2) the storage of iron for intracellular use (providing reserve of iron for cytochromes, nitrogenase, ribonucleotide reductase, hemoglobin, myoglobin); and (3) detoxification in iron excess.<sup>108,109</sup> Expression of ferritin is essential for life which is proved by the early embryonic lethality of ferritin H-chain knock-out mice.<sup>110</sup>

Mammalian cells can obtain iron via multiple routes based on the specific biochemical requirements. Additionally to transferrin-mediated endocytosis, cells can acquire iron complexed with proteins or small molecules. For example, internalization of ferritin via ferritin-specific receptors such as T-cell immunoglobulin and mucin-domain containing protein-2 (TIM-2)<sup>59</sup> or scavenger receptor family class A, member 5 (Scara5) facilitates iron import.<sup>111</sup> Cells can internalize iron indirectly via a heme carrier protein-1, HCP-1.<sup>112</sup> Iron can also be transported from lysosomes to the cytosol by the heme response gene-1, HRG-1.<sup>113</sup>

Cells also express mitochondrial ferritin ( $Ft_{mt}$ )<sup>114</sup> that, similarly to H-ferritin, possesses ferroxidase activity. In contrast to cytosolic ferritin, the expression of  $Ft_{mt}$  is restricted to few tissues and is not iron-regulated.<sup>115</sup>  $Ft_{mt}$  serves as a molecular sink to prevent accumulation of unshielded iron in mitochondria, which protects the organelle against iron's toxicity. The iron storage capacity of  $Ft_{mt}$  is similar to the ubiquitous ferritin; however,  $Ft_{mt}$  has greater avidity for iron<sup>116</sup> and higher iron load when  $Ft_{mt}$  is expressed as a transgene in a cell line.<sup>117</sup>

The presence of ferritin is not limited to the intracellular compartment. It is also found in body fluids, such as serum, cerebral-spinal fluid, and synovial fluids. The origin of the extracellular ferritin may originate from cell damage or from active and regulated ferritin secretion. Assessing the concentration of serum ferritin is a clinically useful index of body iron status. Low serum ferritin levels indicate depleted stores and iron deficient anaemias, whereas increased levels may indicate iron overload. Serum ferritin concentration also increases in inflammation, infection, liver diseases, cancer, and in response to oxidative stress.<sup>88,118</sup>

At high iron loading, ferritin aggregates in the lysosomes to form hemosiderin.<sup>119–121</sup> Hemosiderin is a mixture of ferritin, lipids, and iron<sup>122,123</sup> that is often formed during pathological processes and neurodegenerative diseases associated with altered brain iron metabolism such as Alzheimer's and Parkinson's

diseases, and multiple sclerosis.<sup>124–127</sup> Iron deposition in the brain also increases as a result of the normal aging process, and these changes are detectable by MRI.<sup>128</sup>

## ENDOGENOUS IRON-ASSOCIATED PROTEINS TURNED INTO MRI REPORTERS

The properties of endogenous proteins involved to regulation of the cellular iron content allowed to study those as potential imaging reporters capable in MRI contrast modulation. Examples of genetically encoded iron-associated proteins employed to image of distinct cell populations are shown below.

### Transferrin Receptor

The TfR was the first MRI reporter gene proposed by Koretsky et al. in 1996,<sup>55</sup> based on its function of facilitating metal transport across membranes by internalizing the transferrin-iron complex through receptor-mediated endocytosis.<sup>129</sup> It raises the level of labile iron in the cells, therefore can be used as one potential way to generate MRI contrast. The TfR has a fast rate of turnover ( $2 \times 10^4$  transferrin molecules internalized per minute), which results in the quick uptake of large amounts of iron.<sup>130</sup> The synthesis of the endogenous receptor is tightly controlled through an iron-dependent negative feedback in cells; this provides an adequate supply of the essential metal in function of the iron need, while guarding against toxic excess of iron.<sup>96,131–133</sup> Genetic modification of cells to express a TfR lacking mRNA destabilization motifs leads to constitutively overexpressed high levels of TfR with subsequently increased accumulation of iron in cells, resulting in higher MR contrast.<sup>134</sup>

The TfR is a receptor that can be (over-) expressed in very high numbers (several million copies per cell) on the cell membrane. Fibroblasts overexpressing TfR exhibited an approximately threefold increase in iron content yielding significant MRI contrast in T<sub>2</sub>-weighted sequences.<sup>55</sup> In the absence of iron, the binding sites of transferrin can accommodate a number of other metals including gallium, copper, chromium, cobalt, manganese, vanadium, aluminum, terbium, plutonium, europium, indium, and platinum.<sup>130</sup> The feasibility of manganese labeling of murine hepatocytes via the transferrin-receptor-dependent and/or -independent metal-transport pathways has been documented.<sup>135</sup> This method of cell labeling is based on the chemical similarities between manganese and iron

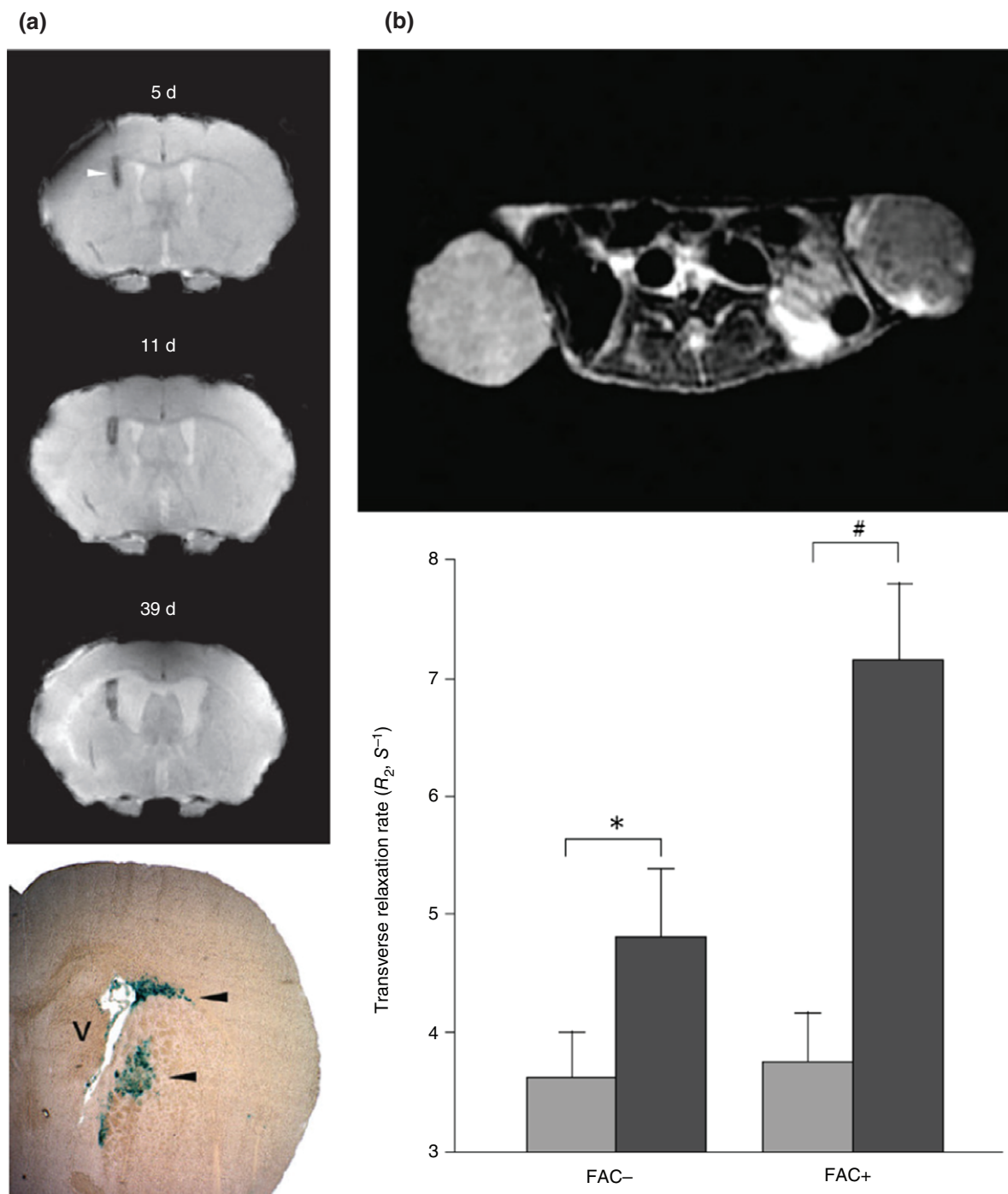


**FIGURE 2** | *In vivo* MRI detection of ferritin expression. (a)  $T_2^*$ -weighted images of the mouse brain at days 5, 11, and 39 after inoculation of an adenovirus containing the MRI reporter ferritin into the striatum. Images were acquired at 11.7 T with a 0.75-mm slice thickness and an in-plane resolution of 102  $\mu\text{m}$ . Bottom image is the Prussian blue staining for iron representing similar pattern to the MRI. v, ventricle (Reprinted with permission from Ref 52. Copyright 2005 Nature). (b) Representative  $T_2$ -weighted images of mice inoculated with tumors over-expressing ferritin heavy chain *in vivo* (right tumor) and parent cells (left). External iron supplementation enhances MRI contrast based on ferritin overexpression. (Reprinted with permission from Ref 136. Copyright 2012 Hindawi)

(e.g., similar ionic radii; similar valence states—(II) and (III)—under physiological conditions; and similar binding affinities for transferrin). The

results of these studies demonstrate that Mn(III)-transferrin is an effective MRI contrast agent for labeling murine hepatocytes.

## Ferritin, Iron Storage Protein

The intracellular level of ferritin can be genetically altered. The higher number of ferritin complexes per cell causes higher iron accumulation, thus directly affecting MRI contrast. The possibility of using ferritin in biomedical imaging and cell labeling was shown in 1992 by Meldrum et al.<sup>98</sup> In 2005 Cohen et al. used ferritin expression and eGFP under tetracycline control to visualize C6 glioma cells transplanted to the mouse.<sup>51</sup> Genove et al. demonstrated the use of ferritin as an MRI reporter gene by injecting an adenoviral vector for transient overexpression of human ferritin (H-chain) into the brain parenchyma of mice, resulting in significant loss of signal at the site of vector injection<sup>52</sup> (Figure 2(a)).

During the last decade, ferritin overexpression has been extensively explored for a variety of applications, such as imaging of transgenic tumors.<sup>51,137,138</sup> Ferritin overexpression has been detected *in vivo* in the mouse brain,<sup>48,52</sup> *in utero* in transgenic mice<sup>139</sup> and in liver hepatocytes.<sup>140</sup> A ferritin shell was used in material science as a precursor for making nano-composite particles as an effective MRI contrast agent for macrophage tracking<sup>141</sup> and for noninvasive imaging of atherosclerosis.<sup>142</sup> Replacing the native iron core in ferritin with a synthetic paramagnetic core<sup>143</sup> has proven to result in effective  $T_2$  relaxation enhancement both *in vitro*<sup>144</sup> and *in vivo*.<sup>145</sup>

Additionally to cell labeling, it was shown that a ferritin expression vector can also be used to monitor *in vivo* gene expression. GL261 mouse glioma cells expressing ferritin–DsRed fusion protein under b-actin promoter showed reduced  $T_2$ -weighted signal intensity for *in vitro* and *in vivo* MRI studies as well as DsRed fluorescence in optical imaging.<sup>138</sup>

First application of mitochondrial ferritin ( $Ft_{mt}$ ) as an MRI reporter has been proposed by Iordanova et al.<sup>146</sup> In that study, mitochondrial ferritin was modified to localize within the cell cytoplasm for efficient iron load and MRI tracking on olfactory sensory neurons.

It is important to emphasize that no exogenous iron supplementation is required for MRI contrast generation by overexpressed ferritin. The fact that ferritin-tagged grafts cause strong signal intensity can be explained only by redistribution of endogenous iron and its accumulation from the host tissue in the overexpressed ferritin complexes.<sup>51,52,80</sup> However, external iron supplementation can enhance MRI contrast based on ferritin overexpression<sup>136</sup> (Figure 2(b)).

To date, several molecular biology approaches and different vectors have been used to overexpress ferritin: adenoviral,<sup>52</sup> retroviral,<sup>51</sup> lentiviral,<sup>54,81,137,147</sup> and adeno-associated virus gene delivery<sup>54</sup>; different plasmid vectors have also been used.<sup>53,57,138,148</sup> The technique chosen for reporter gene expression is crucial as its properties will determine whether contrast generation will be transient or stable, constitutive, inducible, or tissue-specific. Continuous expression is best suited for tracking the survival and the migration of labeled cells. Therefore, several studies investigating MRI reporter genes for long-term tracking of transplanted cells have focused on methods to introduce reporter genes stably into the cells of interest, such as lentiviral (LV) and adeno-associated viral (AAV) vectors for reporter gene expression. AAV-mediated ferritin overexpression through direct vector injection into the brain was shown to be the most promising way for *in vivo* reporter gene imaging in the brain that resulted in significantly enhanced contrast to background on  $T_2^*$ -weighted MRI in comparison with other delivery systems<sup>54</sup> (Figure 3). By introducing a genetic switch, ferritin expression can be turned on or off and changes in the imaging signal can be detected within several days thereafter.<sup>51,140</sup> Being able to control overexpression is important in avoiding potential toxicity issues associated with constitutive overexpression of ferritin, even though overexpression of ferritin results in suppression of the damaging Fenton reaction and thus can protect cells from oxidative damage enhancing the survival of the administered cells.<sup>53</sup> These results suggest that ferritin holds significant promise as translational MRI reporter gene for *in vivo* imaging of live transplanted cells.

## Bacterial Magnetosome-Associated MRI Reporters (*magA* and *mms6*)

Iron-associated biomolecules were found not only in mammalian cells, but also in bacteria, and explored as potentially interesting MRI reporter genes. Formation of iron biominerals is a naturally occurring phenomenon among magnetotactic bacteria which produce magnetite ( $Fe_3O_4$ ) in a subcellular compartment termed the magnetosome. There are two main components to the magnetosome: the biomineral and the lipid bilayer that surrounds it. Magnetotactic bacteria naturally synthesize these intracellular magnetic structures which help to direct motility of the bacteria based on the earth's magnetic field.<sup>149,150</sup> The magnetosome-associated proteins are important for vesicle formation, cytoskeletal attachment, iron transport, and crystallization.<sup>151</sup> Expression of magnetosome genes in nonbacterial cells

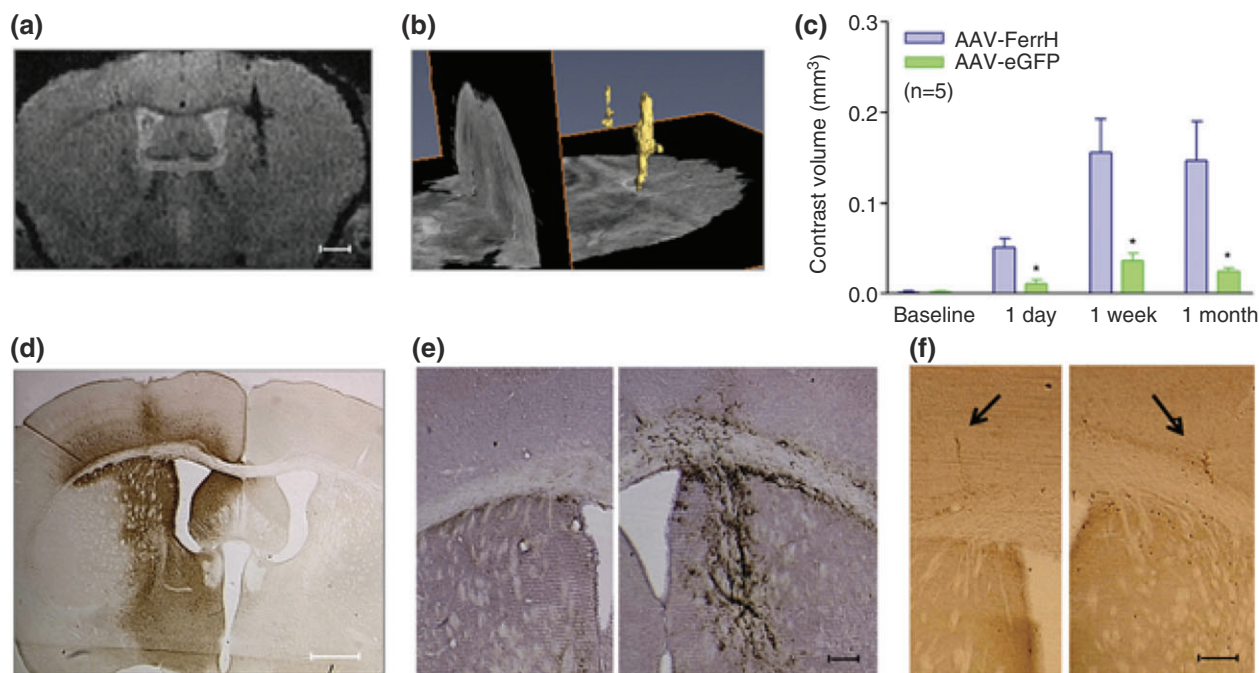


**FIGURE 3** | AAV-FerrH-mediated contrast evaluation by MRI. (a) 3D  $T_2^*$ -weighted *in vivo* MR image acquired 1 month after injection of AAV-FerrH-T2A-fluc and AAV-eGFP-T2A-fluc vectors in the right and left striata, respectively. (b) 3D graphic representations of the contrast volume from the same mouse. (c) Quantification of the contrast volume using the normalized 3D  $T_2^*$ -weighted *in vivo* MR images at different time points post-injection. (d) Immunohistochemical staining for eGFP shows a large area of transgene expression after AAV transduction in the brain. (e) DAB-enhanced Prussian blue staining, showing the presence of iron at the site of AAV-FerrH injection in contrast to the contralateral control injection site where very little iron is detectable. (f) immunohistochemical staining on an adjacent section using CD11b antibody, showing very few CD11b-positive cells at the left and right injection tracts (arrows). White scale bars represent 500 mm, black scale bars 100 mm. (Reprinted with permission from Ref 54. Copyright 2011 Nature)

provides new opportunities for development of reporter gene-based contrast for MRI.

Based on the involvement of *magA* in the synthesis of magnetosomes in *Magnetospirillum* bacterial species,<sup>152–154</sup> the use of this gene has been explored as an inducer of MRI-detectable contrast. It has been shown that *magA* can be expressed in mammalian cells and its expression leads to the formation of magnetic nanoparticles that strongly affect the MRI signal<sup>155</sup> (Figure 4). However, it is not yet known whether *magA* expression leads to the formation of the same iron oxide crystals seen in magnetotactic bacteria. MRI detection of *magA* expression has been shown in mouse neuroblastoma (N2A) cells<sup>156</sup> and in the human 293FT cell line.<sup>155</sup> The iron-based MRI reporter *magA* resulted in larger increase in  $R_2$  relaxation: cell pellets expressing *magA* consistently showed an increase in  $R_2$  of approximately three- to fourfold,<sup>155</sup> comparing to an increase in  $R_2$  of approximately 2.5-fold for ferritin expression.<sup>52</sup>

*Escherichia coli* expressing *magA* showed increased iron uptake in membrane vesicles when

cells were supplemented with iron and ATP. However, this response was limited when ATP was excluded, suggesting that *magA* function is coupled to ATP hydrolysis.<sup>157</sup> *MagA* might be expressed in a controllable fashion using a doxycycline-inducible promoter.<sup>155</sup> This has the advantage that reporter gene expression can be switched on or off, which is important for controlling *magA* expression levels in order to avoid cytotoxic effects at high levels of overexpression.<sup>158</sup> *In vivo*, *magA* overexpression did not lead to pathological alterations in transgenic mice and could even attenuate oxidative damage due to iron overload.<sup>159</sup> An additional iron supplementation of *magA*-expressing cells increased transverse relaxation rates compared to nonsupplemented cells,<sup>160</sup> also *in vivo*.<sup>159</sup> It was shown that expression of both magnetotactic bacterial gene *magA* and mammalian iron storage protein ferritin in MDA-MB-435 tumor cells sequestered iron within a membrane-enclosed vesicle and permitted iron biomineralization with simultaneous regulation of mammalian iron homeostasis.<sup>160</sup> These results highlight the potential of magnetotactic bacterial gene expression for improving



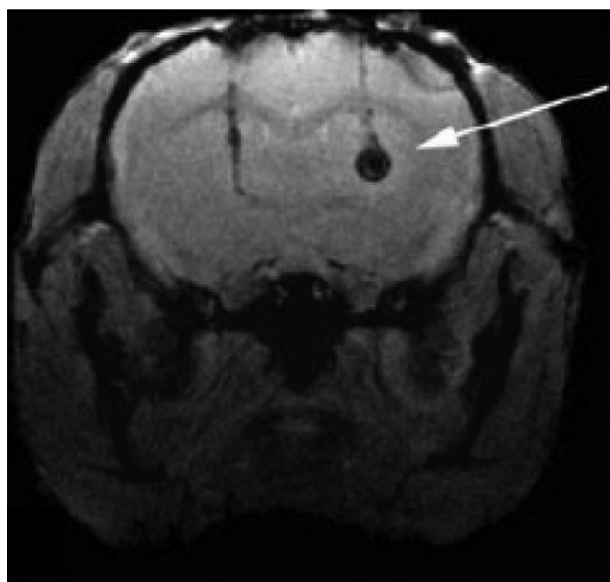


**FIGURE 4** |  $T_2^*$ -weighted image of mouse brain with transplanted *magA* cells (right) and GFP control cells (left) after 5 days of induction. These cells were neither induced nor incubated with iron supplement prior to transplantation. The *magA* cells (white arrow) exhibit significantly lower MRI signal, reflecting an increase in  $R_2$ , suggesting that *magA* cells are able to use endogenous iron sources. The control cells on the left do not show such an effect. (Reprinted with permission from Ref 155. Copyright 2008 Harvard Catalyst)

MR contrast. However, *magA*'s status as a putative MR reporter gene is controversial as its implication in magnetosome formation has been contested.<sup>154</sup>

Another bacterial gene, magnetosome-associated *mms6*, has been proposed as a reporter gene for MRI of mammalian cells.<sup>161</sup> *In vitro* experiments show that *mms6*-expressing cells form clusters of nanoparticles within and outside membrane-enclosed structures and produce changes in MR contrast, most likely by increasing iron uptake of intracellular iron. *In vivo* MRI experiments demonstrate that *mms6*-expressing tumors can be distinguished from parental tumors not expressing *mms6*, even in the absence of exogenous iron supplementation. Whether *mms6* is an efficient genetic MR reporter remains to be established, and potential toxicity issues should be clarified. *Mms6* protein fused to the C-terminal of murine h-ferritin has been proposed as a novel chimeric magneto-ferritin reporter gene—ferritin-M6A, enabling magnetite biomineralization of ferritin and enhancing  $R_2$  relaxivity of ferritin-M6A-expressing C6-glioma cells.<sup>162</sup>

### Timd2, Mediator of Ferritin Endocytosis

T-cell immunoglobulin and mucin domain containing protein receptor (Timd2 or Tim-2) are expressed

primarily on immune cells, where it plays a role in signaling and mediates ferritin endocytosis.<sup>59,60,163</sup> Timd2 expression elsewhere is limited, but is also found in both liver and kidney, where it functions primarily as a ferritin receptor to remove ferritin from the blood,<sup>59</sup> as well as on oligodendrocytes, where it is upregulated during myelination to meet increased iron demands.<sup>60</sup> It has been shown that cells expressing Timd2 and incubated with ferritin or manganese-loaded apoferritin showed large increases in  $R_2$  and  $R_1$ , respectively. Cells expressing Timd2 implanted as xenografts in mice also showed changes in  $R_2$  following intravenous injection of ferritin, although these changes in contrast were more modest than those observed *in vitro*.<sup>61</sup> Therefore, Timd2 represents another potential MRI-based gene reporter.

## CELL-TRACKING APPLICATIONS

### Neural Stem Cell Migration

It was a long-standing paradigm that brain damage occurring during adulthood is irreparable, until this paradigm started shifting with the discovery of neural stem-like cell pools residing in discrete brain regions.<sup>170</sup> When active populations of neural stem cells (NSC) were also found to generate new neurons in the adult human brain,<sup>171</sup> hope was raised that possible stimulation of this endogenous stem cell pool could have the potential for neuro-regenerative therapy after brain injury, without having to transplant exogenous cells. Because the often invasive standard methods used to monitor the proliferation, migration, differentiation, and functional integration of endogenous NSCs and their progeny are limited in studying dynamic processes, novel techniques and contrast mechanisms for *in vivo* imaging of neurogenesis have been developed and successfully applied.<sup>172</sup> *In vivo* labeling of endogenous neuronal progenitor cells *in situ* with magnetic nanoparticles has proven useful for tracking neuroblast migration with MRI,<sup>173–178</sup> but only labeling with genetic reporters can overcome the issues with dilution of contrast agents and subsequent signal loss upon cell division and has potential for long-term monitoring of neurogenesis. Using LVs expressing ferritin to label the endogenous NSCs, the stem cell progeny migrated and integrated in the olfactory bulbs could be detected and quantified with *ex vivo* MRI, but for *in vivo* tracking of the migrating stem cell progeny, the system lacked sensitivity.<sup>48</sup>

In search of improving the contrast generating properties of ferritin, linking the light and heavy

chains of ferritin resulted in a slightly larger protein cage and improved MR contrast *in vitro*.<sup>147</sup> Using an adenoviral vector encoding this chimeric ferritin reporter to label endogenous neural progenitor cells, migrating cells could be visualized along the rostral migratory stream with *in vivo* MRI at 11.7T.<sup>179</sup> However, no contrast was seen in the olfactory bulbs where these cells arrive and integrate. Although possibly due to the vector system used for gene transfer, improving the sensitivity of ferritin nevertheless remains a challenge. The strategy to combine constitutive overexpression of both ferritin heavy chain and the TfR in mouse NSCs implanted into the mouse brain did not lead to spectacularly improved results<sup>57</sup> (Figure 5). This work provides an example of how gene reporter-based contrast improves at 7T in comparison with the standard clinical field strength of 1.5 T.

## Heart

Molecular and cellular imaging is essential in the evaluation of graft survival and cardiac repair after cell transplantation. Myocardial infarction leads to significant loss of cardiomyocytes, scar formation, and impaired contractile function. Since the heart has very limited intrinsic regenerative capabilities, transplantation of new cardiomyocytes offers a promising treatment approach. MRI is the perfect imaging modality for noninvasive visualization of soft tissues. It is valuable for assessment of heart contractile function, chamber morphology, vascularity, inflammation, infarct size, tissue viability, metabolism, as well as for evaluation of the transplanted cell localization and graft size. Most of the cell tracking studies have been done using SPIOs nanoparticles that provide robust MR signal detection, useful for short-term monitoring of cell localization and migration. It

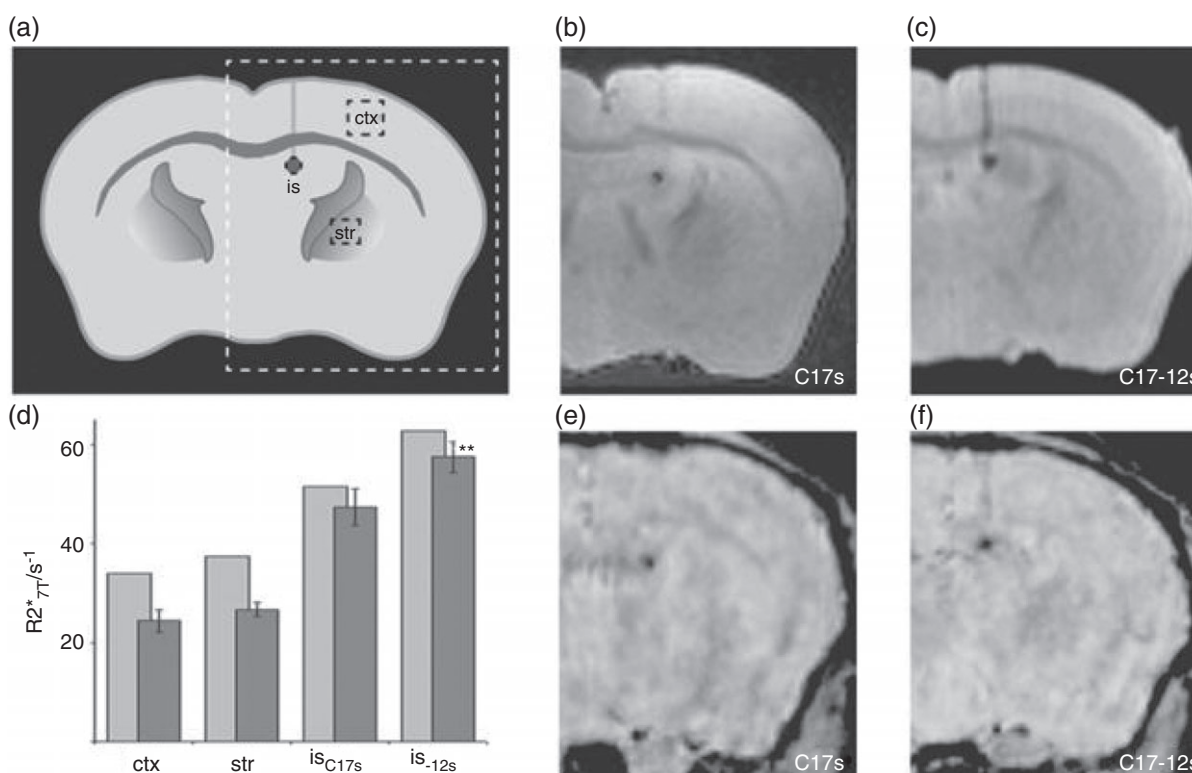


**FIGURE 5** |  $T_2^*$ -weighted MR images of mouse brain at 7T and changes in  $R_2^*$  relaxivity in transgenic cell samples. (Reprinted with permission from Ref 57. Copyright 2006 Wiley) (a) Schematic of a coronal section of an adult mouse brain shows the location of the MRI images (b, c, e, and f) shown, including the injection site (is), and control regions in cortex (ctx), and striatum (str).  $T_2^*$ -weighted images from *ex vivo* mouse brains injected with C17s control cells (b) or C17-12s transgenic cells (c) clear contrast between the transplanted cells and surrounding brain tissue. (d) Mean  $R_2^*$  measurements (dark bars) were made on *ex vivo* brains for ROIs within the injection site of either the C17s injected brains or the C17-12s injected brains, as well as for region of interest (ROIs) within ctx and str. Error bars denote the SD in each case.  $R_2^*$  was significantly increased in is-12s versus isC17s (\*\* $P < 0.04$ ). Light bars indicate the  $R_2^*$  values measured in the same regions from an *in vivo* multi-GE acquisition of a C17s injected brain and a C17-12s injected brain. *In vivo*  $T_2^*$ -weighted images from C17s (e) and C17-12s transplanted mice (f) were acquired from mice later used in *ex vivo* imaging (data included in b and c, respectively).

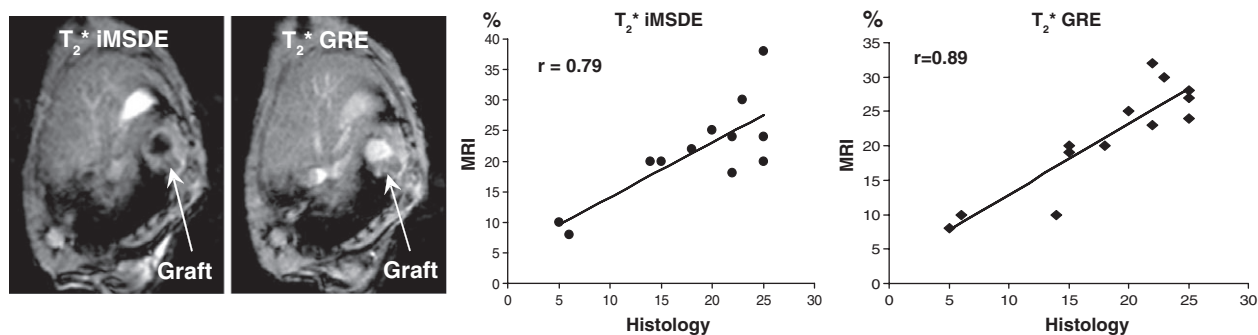


**FIGURE 6** | MRI detection of ferritin-tagged graft in the infarcted mouse heart using  $T_2^*$  iMSDE and  $T_2^*$  GRE pulse sequences and correlation of the graft size measurements between MRI and histology (Reprinted with permission from Ref 80. Copyright 2012 Wiley).

has been shown that direct injection of cells into the myocardium is the most effective delivery for heart repair.<sup>180</sup> Gene reporter expression is better suitable for longitudinal follow-up of changes in graft size and viability. *In vivo* MRI detection of cardiac grafts overexpressing ferritin in infarcted mouse hearts was shown to be feasible.<sup>53,68,80</sup> MRI thereby provided morphological measurements of graft size with reasonable accuracy and precision<sup>53,80</sup> (Figure 6).

In the context of longitudinal graft imaging, the MRI contrast provided by ferritin over-expression does not diminish with cell proliferation and represents live grafted cells, while imaging signal from iron-oxide particles is not related to graft viability and size, but may be a better marker for high-resolution detection of cell location by MRI.<sup>68,181</sup>

Campan et al. employed ferritin expressing swine cardiosphere-derived cells for serial imaging on a 1.5 T MRI scanner after transplantation to a rat model of myocardial infarction.<sup>182</sup> The hypointense signal on MRI was detectable at 1 week after infarction and its size did not change significantly after 4 weeks,<sup>182</sup> which is a surprising finding since immune rejection of the pig cells is expected in Wistar rats. Prussian blue staining confirmed the presence of differentiated, iron-accumulating cells containing mitochondria of porcine origin.

An example of plasma membrane bound contrast complexes was described for cardiac applications of ESCs engineered to express the reporter proteins myelocytomatosis (myc) and hemagglutinin (HA) and transplanted into infarcted myocardium in mice. Regions of surviving/proliferating ESC were detected on  $T_2^*$ -weighted images following intravenous injection of iron oxide nanoparticles conjugated to either anti-myc, or anti-HA monoclonal antibodies. Further, by spacing follow-up scans appropriately to allow for washout of labeled SPIO particles, a clear time-course of proliferation and teratoma formation was determined.<sup>71</sup> The combination of a

gene-expression- and particle-based cell labeling approaches may help to overcome the limitations of each individual labeling technique.

## Tumors

Molecular imaging has already become an indispensable tool in basic oncology research to identify not only tumor location and size, but also critical biological pathways involved in oncogenesis and cancer progression.<sup>183</sup> Most cancer imaging has been done with optical and nuclear imaging technology, whereas MRI and MR spectroscopy have been used for assessment of nanomedicine-based strategies for cancer treatment and in image-guided enzyme/prodrug cancer therapy.<sup>184,185</sup> MRI gene reporters, such as ferritin and transferrin, have mostly been assessed in tumor models as proof-of-principle approach. Tetracycline-controlled ferritin overexpression for MRI visualization was demonstrated in a tumor formed by C6 glioma cells. Inoculation of these tumor cells in nude mice revealed a significant decrease in  $T_2$  on tetracycline withdrawal<sup>51</sup> (Figure 7, study 1). In studies of Moore et al.<sup>56,134</sup> and Weissleder<sup>186</sup> 9L gliosarcoma cells were genetically engineered to express human TfR (hTfR). It was demonstrated that a conjugate of transferrin and monocrySTALLINE iron oxide nanoparticles can be used for amplification of receptor expression and MRI visualization in this model (Figure 7, study 2). MCF-7 and F-98 cells could be tagged by a bimodal lentiviral vector encoding myc-tagged human ferritin and green fluorescent protein. These transgenic tumors had significantly decreased  $T_2$  and  $T_2^*$  relaxation times on 1.5T MRI, 1–4 weeks after transplantation in mice and rats<sup>137</sup> (Figure 7, study 3). Subcutaneous teratoma formation in nude mice was imaged at the 4.7 T magnet at 14 and 21 days post inoculation of mouse stem (mES) cells expressing ferritin<sup>81</sup> (Figure 7, study 4). The added value of increased MRI contrast for the detection of solid tumors in these studies remains unclear, but the low level of contrast generated by the reporter genes

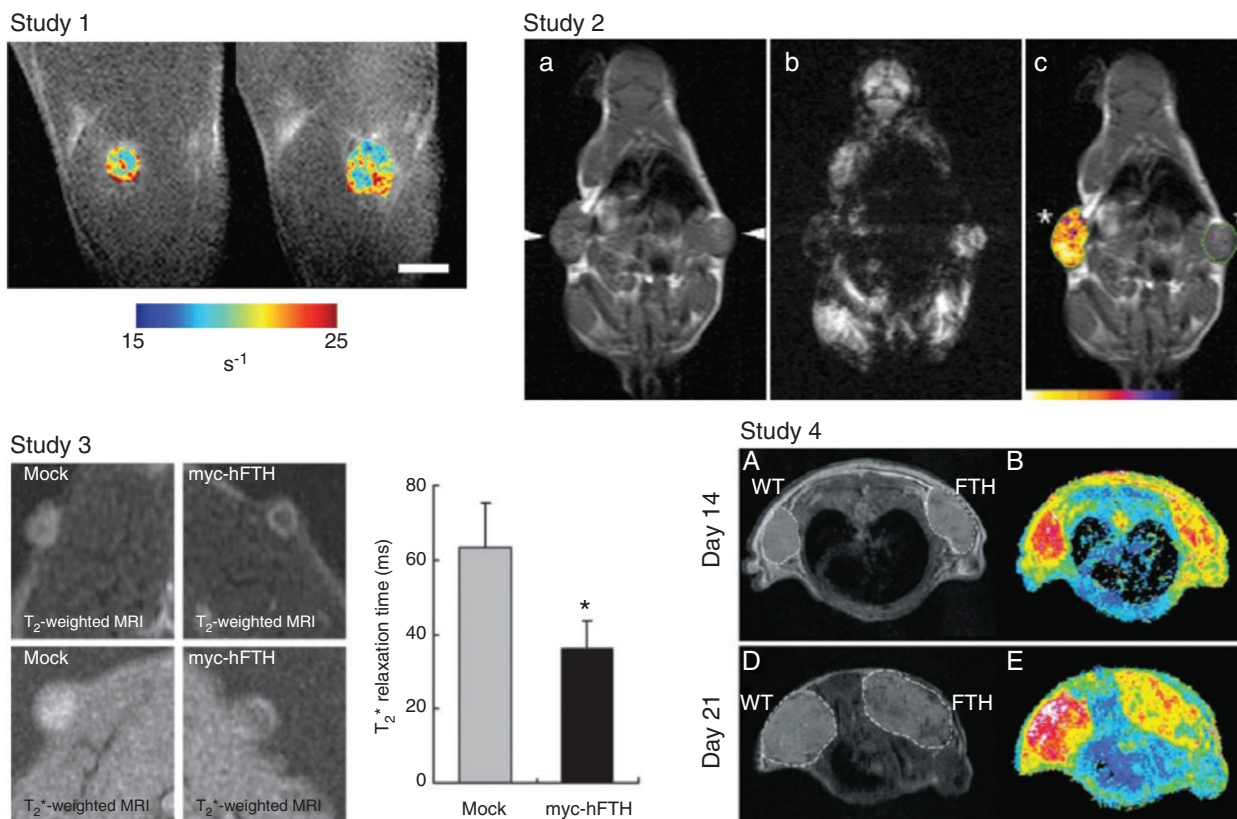


**FIGURE 7** | MR imaging of iron-oxide reporters in cancer applications. Study 1: *In vivo*  $R_2$  maps of C6 tumors expressing ferritin in hind limb of CD1-nude mice. Scalebar 2.5 mm (Reprinted with permission from Ref 51. Copyright 2005 Elsevier). Study 2: *In vivo* MRI of a mouse with transplanted gliosarcoma cells expressing human transferrin receptor (left arrowheads) and naïve (right arrowheads) flank tumors. (a)  $T_1$ -weighted coronal spin-echo image. (b)  $T_2$ -weighted gradient-echo image corresponding to the image in (a). Transferrin-mediated cellular accumulation of the superparamagnetic probe decreases signal intensity. (c) Composite image of a  $T_1$ -weighted spin-echo image obtained for anatomic detail with superimposed  $R_2$  changes after Tf-MION administration, as a color map (Reprinted with permission from Ref 186. Copyright 2000 Nature). Study 3: *In vivo*  $T_2$ - and  $T_2^*$ -weighted MRI of F-98 tumor 2 weeks after subcutaneous transplantation of myc-hFTH and mock cells (left) and  $T_2^*$  relaxation times of mock and myc-hFTH tumors were measured from  $T_2^*$ -weighted images (right) (Reprinted with permission from Ref 137. Copyright 2010 AACR). Study 4: *In vivo* MRI detection of FTH transgene-induced MRI contrast in mES cell grafts. (A, D) Representative  $T_2$ -weighted fast spin echo (FSE) images showing the same pair of tumors grown from mES grafts (left, WT; right, FTH transgenic), at days 14 and 21 postinoculation. (B, E) Corresponding color-coded  $T_2$  maps from multiecho measurements of  $T_2$  relaxation time showed significant reduction of  $T_2$  relaxation time in the tumor overexpressing FTH transgene at both time points (Reprinted with permission from Ref 81. Copyright 2009 Mary Ann Liebert Inc).

makes the use of MRI for tracking of metastatic cancer cells highly unlikely.

Gene reporter imaging has its advantages for longitudinal monitoring of tumor growth without the need for external administration of contrast agents or concerns over signal loss over cell division. However, biomedical applications might be limited to preclinical research on animals, since transgenic manipulations are required for creation of stable cell lines.

## CHALLENGES, LIMITATIONS, AND IMPROVEMENT STRATEGIES

Despite the significant value that reporter gene imaging brings to the field of molecular imaging and cell

tracking with MRI, there are several limitations and challenges that remain to be resolved and that warrant further research attention before the reporter gene-based contrast paradigm can be exploited to its full potential for MRI applications.

### Low Sensitivity

The low sensitivity of MRI compared to other modalities in visualization of reporter genes remains a major challenge. The majority of iron-associated MRI gene reporters are yielding imaging signal attenuation rather than signal gain. Detection of those signals requires development of complicated time-consuming acquisition and processing protocols.<sup>187–193</sup> Many technical and methodological

improvements, such as higher field strength, dedicated RF coils, superconducting RF coils, and new pulse sequences could be implemented for substantial improvements of signal detection generated by iron-associated MRI reporters. In contrast to genetic cell labeling, synthetic iron oxide nanoparticles, possess much higher  $R_2^*$  relaxivity, enabling *in vivo* MRI tracking of a single cell,<sup>194</sup> which is a level of sensitivity not possible with native and engineered reporter gene cell labeling. Further improvements in MRI sensitivity for reporter gene detection are possible, by intensifying the MRI signal by external iron supplementation,<sup>136</sup> by transferrin labeled contrast media<sup>186</sup> or by manipulating mineralization and engineering of mutant ferritin proteins.<sup>102</sup> A chimeric ferritin with a fixed subunit stoichiometry by fusion of the L and the H subunits (L\*H and H\*L) was created and improved the sensitivity of MRI for ferritin detection to some extent.<sup>147</sup> Cellular MRI contrast could also be slightly enhanced via co-expression of the TfR and ferritin.<sup>57</sup> The modulation of ferritin aggregation by binding to cytoskeletal elements might be another useful strategy to increase transverse relaxivity.<sup>195</sup> Another way to enhance MRI sensitivity of gene reporter imaging is to combine expression of specific genes with targeted delivery of iron oxide nanoparticles and increased iron storage within selected cells. For example, intravenous administration of holo-transferrin covalently bound to iron oxide nanoparticles generated significant contrast on  $T_2^*$ -weighted images in cells overexpressing transferrin,<sup>186,196,197</sup> or the administration of antibody-tagged SPIOs targeted to tag sequences expressed on transplanted stem cells into infarcted heart,<sup>71</sup> as we mentioned above. Taken together, the sensitivity of reporter gene induced contrast for MRI remains limited for cell tracking applications, in particular for those involving small population sizes. More sensitive MRI reporters, and particularly those that would help to gain the signal rather than attenuating it, would be a significant advance in this field. Examples pursuing such an approach are all based on uptake of manganese or gadolinium-based agents that enhance  $T_1$  contrast, rather than iron-oxide-based contrast that modulates the  $T_2$ .<sup>58,198,199</sup>

### MRI Signal Specificity Issues

MRI contrast based on iron-associated reporter gene overexpression may also suffer from specificity issues when the endogenous ferritin or iron content is elevated.<sup>200,201</sup> Signal specificity issue is generally pertains to any cell labeling strategies based on negative contrast. The signal void caused by iron accumulation

is almost indistinguishable in MRI from that caused by hemosiderin deposition in the damaged tissues<sup>80,202,203</sup> or hemorrhage caused by needle insertion to the brain.<sup>201</sup> Under pathological conditions, the total amount of tissue iron and the proportion stored as hemosiderin can increase, while the capacity of ferritin to store iron is overwhelmed.<sup>99,107,204,205</sup> Therefore, hemosiderin deposition areas may obscure contrast from iron-associated reporter gene expression.<sup>80,202,203,205</sup> Care should therefore be taken with interpretation of areas of signal void is, especially for small grafts that cannot be precisely identified by a known anatomical location. These limitations could potentially be overcome by the application of technical approaches, such as analysis of non-monoexponential signal decay,<sup>187–189</sup> advanced acquisition modes<sup>190,191</sup> or postprocessing methods<sup>192,193</sup> that enable generation of positive contrast in the presence of paramagnetic materials, such as iron oxides. Although DNA and protein degradation occur rapidly after cell death,<sup>206</sup> there are no data as to how rapidly ferritin complexes undergo degradation after the death of transplanted cells and for how long the MRI signal from iron persists. Cessation of *magA* induction resulted in a return of iron content in 293FT cells to control values within 6 days, suggesting activation of iron degradation pathways.<sup>155</sup> It will be important to determine how quickly other iron-associated proteins can be produced by daughter cells and how quickly ferritin complexes can bind a sufficient amount of iron from the extracellular environment to be detected by MRI.

### Administration of Cells

One of the challenges in imaging of transplanted cells is their administration route. Cell therapies ideally involve systemic administration of cells with subsequent homing of cells to the site of injury. Nevertheless, systemically administered cells distribute to multiple organs with primary localization to the lungs, liver, spleen, or marrow spaces and relatively few cells homing to diseased sites.<sup>207–209</sup> For these applications where low cell numbers are to be found, MR reporter genes are unlikely to be adequate labels given their low sensitivity. All published MR reporter gene studies to date involved a bolus injection of transgenic cells or viral agent into a target organ with subsequent accumulation of labeled cells. Direct injection of a labeling agent allows local distribution and higher concentration of the label, needed for robust MRI detection. While preclinical cardiovascular and cancer models utilized concentrated injections of large numbers (millions) of cells, the typical

injections in neurological studies utilize orders of magnitude less cells (thousands), presenting a potential sensitivity barrier to the use of MRI reporter genes for neurological studies. In this case, as well as for imaging of cells administered systemically, synthetic nanoparticles remain the more suitable option for short-term MRI tracking due their higher iron payload.

### Expression Level

The site of transgene insertion in the genome and the number of transgene copies can significantly affect the expression level. Use of novel cloning techniques, such as zinc finger nuclease (ZFN),<sup>210–212</sup> clustered regulatory interspaced short palindromic repeats (CRISPR)<sup>213,214</sup> or transcription activator-like effector nucleases (TALENs)<sup>215</sup> would make transgene insertion targeted to a specific locus in the chromosomes. Targeted genome addition can provide persistent expression of the transgene while avoiding gene silencing and insertional mutagenesis caused by viral vector-mediated random integration. ‘Safe harbours’ can be chosen for insertion of a transgene, such as ROSA26<sup>216</sup> or AAVS1.<sup>217,218</sup> To direct transgene integration, ZFN and TALENs methods use DNA-binding modules engineered to match a target DNA sequence. The CRISPR system uses RNA-guided Cas9 DNase activity to generate sequence-specific target cleavage.<sup>214</sup>

### Safety

The toxicity and interference associated with any cell label or expressed reporter gene should be addressed carefully. Reported changes in the cell’s phenotype either accompanied with or without alterations in proliferation or viability, do raise concerns about possible toxic effects of iron-associated gene overexpression.<sup>57,200,219,220</sup> For example, chronic overexpression of H-ferritin (FTH1) in a transgenic mouse resulted in progressive age-related neurodegeneration.<sup>221</sup> The constitutive expression of *magA* from *Magnetospirillum magnetotacticum* was tolerated by human embryonic kidney (HEK) cells but induced a strong toxic effect in murine mesenchymal/stromal cells and kidney-derived stem cells, restricting its use as a reporter gene.<sup>200</sup> As an alternative solution to constitutive expression, an inducible system might be advantageous: controllable expression of gene reporter can minimize the adverse effects of constitutive expression (e.g., toxicity, reduced proliferation rate, possible impact on differentiation potential). Another solution is addition of suicide genes, such as

herpes simplex virus type 1 thymidine kinase (HSV1-tk), for targeted deletion of the transplanted cells in case of adverse effects.<sup>222,223</sup>

For longitudinal studies of proliferation, migration, differentiation, and functional integration of therapeutic cells, long-term safety and stability are required. Applications of gene reporters in clinical studies are still problematic because of the concerns regarding potential toxicity and tumorigenicity of transgenic manipulations with cells. In this context, the development of novel imaging methods that could provide alternative contrast properties capable of identifying specific cell types is of particular interest. Recently, several MRI methods exploiting endogenous contrast-generation mechanisms were proposed. For example, chemical exchange saturation transfer (CEST) contrast agents can identify the presence of certain enzymes, and their application holds great promise in potential ‘multi-color’ MRI.<sup>31–33</sup> Another method, based on macromolecular proton fraction (MPF) mapping is determining the relative amount of immobile macromolecular protons involved in magnetization exchange with mobile water protons and can provide quantitative information about tissue composition and collagen content.<sup>224</sup>

### Imaging Multimodality

Multimodal imaging approaches seem the most interesting option to overcome limitations of individual imaging techniques regarding specificity, sensitivity, tissue penetration, etc. There is an enormous yet so far under-exploited potential for synergy by combining the strengths of different approaches available. In this view, future perspectives behold the combined visualization of processes with different reporter genes with different functions integrated in one expression cassette.

### FUTURE DIRECTIONS

Molecular imaging technology provides invaluable tools for researchers to study transplanted cells non-invasively: their survival, engraftment, proliferation, and possible mechanisms of benefit. Despite the extensive use of reporter genes in preclinical studies, application of molecular imaging in clinical trials is limited. The main obstacle for implementation of the reporter gene imaging for cell tracking in patients is the lack of regulatory confidence in the safety and specificity of genomic manipulations. Additional studies are needed to proof the safety and understanding of the long-term behavior of transplanted

cells with integrated transgenes. Noninvasive imaging can provide quantitative and qualitative assessment of transplanted cell dynamics that would lead to personalized patient care. Functional outcome after cell transplantation is dependent on several aspects, including engraftment success, graft survival, structural, and functional integration within the host tissue. Noninvasive imaging can help to define the optimal cell type, delivery method and time, changes in host microenvironment as well as provide information about off-target behavior and oncogenic events. A particle-based cell labeling is most useful for short-term cell visualization with MRI, for confirmation of the targeted delivery and tracking of cell migration, while a reporter gene approach offers longitudinal monitoring of transplanted cell viability,

proliferation, and migration. To minimize safety concerns, human natural iron-associated proteins, such as ferritin, might be used, or advanced MRI techniques based on endogenous proton exchange contrast mechanisms, such as CEST or MPF, might be implemented for patient trials. Selection of the optimal labeling technique and imaging modality will depend on the studied cellular processes. Since each imaging modality has its own strengths and limitations, a multimodal imaging approach with multimodal gene reporters integrated in one expression cassette might be a potential solution for tracking the fate of transplanted cells and functional benefits. Future studies will likely employ advanced imaging technology to patient's benefits ensuring cell therapy efficacy and safety.

## ACKNOWLEDGMENTS

Authors Drs. Naumova and Vande Velde contributed equally to this work. We thank Dr. Vasily Yarnykh (Research Associate Professor, Department of Radiology, University of Washington, Seattle, WA) for helpful discussions and Zachary Miller (Vascular Imaging lab, University of Washington, Seattle, WA) for proofreading of the manuscript. The manuscript preparation was supported, in part, by the Russian Science Foundation (project No. 14-45-00040). GVV is a postdoctoral fellow of the Flemish Research Foundation (FWO) and acknowledges KU Leuven (StG/15/024) and FWO (1506114N) funding.

## REFERENCES

1. Thomas ED, Lochte HL Jr, Lu WC, Ferrebee JW. Intravenous infusion of bone marrow in patients receiving radiation and chemotherapy. *N Engl J Med* 1957, 257:491–496.
2. Harrison JH, Merrill JP, Murray JE. Renal homotransplantation in identical twins. *Surg Forum* 1956, 6:432–436.
3. Bianco P, Cao X, Frenette PS, Mao JJ, Robey PG, Simmons PJ, Wang CY. The meaning, the sense and the significance: translating the science of mesenchymal stem cells into medicine. *Nat Med* 2013, 19:35–42.
4. Laflamme MA, Murry CE. Heart regeneration. *Nature* 2011, 473:326–335.
5. Li H, Chen G. In vivo reprogramming for CNS repair: regenerating neurons from endogenous glial cells. *Neuron* 2016, 91:728–738.
6. Chong JJ, Yang X, Don CW, Minami E, Liu YW, Weyers JJ, Mahoney WM, Van Biber B, Cook SM, Palpant NJ, et al. Human embryonic-stem-cell-derived cardiomyocytes regenerate non-human primate hearts. *Nature* 2014, 510:273–277.
7. Kawamura T, Miyagawa S, Fukushima S, Maeda A, Kashiyama N, Kawamura A, Miki K, Okita K, Yoshida Y, Shiina T, et al. Cardiomyocytes derived from MHC-homozygous induced pluripotent stem cells exhibit reduced allogeneic immunogenicity in MHC-matched non-human primates. *Stem Cell Rep* 2016, 6:312–320.
8. Doi D, Samata B, Katsukawa M, Kikuchi T, Morizane A, Ono Y, Sekiguchi K, Nakagawa M, Parmar M, Takahashi J. Isolation of human induced pluripotent stem cell-derived dopaminergic progenitors by cell sorting for successful transplantation. *Stem Cell Rep* 2014, 2:337–350.
9. Chung S, Moon JI, Leung A, Aldrich D, Lukianov S, Kitayama Y, Park S, Li Y, Bolshakov VY, Lamonerie T, et al. ES cell-derived renewable and functional midbrain dopaminergic progenitors. *Proc Natl Acad Sci USA* 2011, 108:9703–9708.
10. Horie N, Hiu T, Nagata I. Stem cell transplantation enhances endogenous brain repair after experimental stroke. *Neurol Med Chir* 2015, 55:107–112.
11. Strauss S. Geron trial resumes, but standards for stem cell trials remain elusive. *Nat Biotechnol* 2010, 28:989–990.
12. Kawabata S, Takano M, Numasawa-Kuroiwa Y, Itakura G, Kobayashi Y, Nishiyama Y, Sugai K, Nishimura S, Iwai H, Isoda M, et al. Grafted human

- iPS cell-derived oligodendrocyte precursor cells contribute to robust remyelination of demyelinated axons after spinal cord injury. *Stem Cell Rep* 2016, 6:1–8.
13. Schwartz SD, Hubschman JP, Heilwell G, Franco-Cardenas V, Pan CK, Ostrick RM, Mickunas E, Gay R, Klimanskaya I, Lanza R. Embryonic stem cell trials for macular degeneration: a preliminary report. *Lancet* 2012, 379:713–720.
  14. Schwartz SD, Regillo CD, Lam BL, Elliott D, Rosenfeld PJ, Gregori NZ, Hubschman JP, Davis JL, Heilwell G, Spirn M, et al. Human embryonic stem cell-derived retinal pigment epithelium in patients with age-related macular degeneration and Stargardt's macular dystrophy: follow-up of two open-label phase 1/2 studies. *Lancet* 2015, 385:509–516.
  15. Plaza Reyes A, Petrus-Reurer S, Antonsson L, Stenfelt S, Bartuma H, Panula S, Mader T, Douagi I, Andre H, Hovatta O, et al. Xenofree and defined human embryonic stem cell-derived retinal pigment epithelial cells functionally integrate in a large-eyed preclinical model. *Stem Cell Rep* 2016, 6:9–17.
  16. Hayashi R, Ishikawa Y, Sasamoto Y, Katori R, Nomura N, Ichikawa T, Araki S, Soma T, Kawasaki S, Sekiguchi K, et al. Co-ordinated ocular development from human iPS cells and recovery of corneal function. *Nature* 2016, 531:376–380.
  17. Takebe T, Sekine K, Enomura M, Koike H, Kimura M, Ogaeri T, Zhang RR, Ueno Y, Zheng YW, Koike N, et al. Vascularized and functional human liver from an iPSC-derived organ bud transplant. *Nature* 2013, 499:481–484.
  18. Crunkhorn S. Diabetes: human iPSC-derived  $\beta$ -like cells rescue diabetic mice. *Nat Rev Drug Discov* 2016, 15:382–383.
  19. Massoud TF, Gambhir SS. Molecular imaging in living subjects: seeing fundamental biological processes in a new light. *Genes Dev* 2003, 17:545–580.
  20. Naumova AV, Modo M, Moore A, Murry CE, Frank JA. Clinical imaging in regenerative medicine. *Nat Biotechnol* 2014, 32:804–818.
  21. Chen IY, Wu JC. Cardiovascular molecular imaging: focus on clinical translation. *Circulation* 2011, 123:425–443.
  22. Kooreman NG, Ransohoff JD, Wu JC. Tracking gene and cell fate for therapeutic gain. *Nat Mater* 2014, 13:106–109.
  23. Nguyen PK, Riegler J, Wu JC. Stem cell imaging: from bench to bedside. *Cell Stem Cell* 2014, 14:431–444.
  24. Cho IK, Wang S, Mao H, Chan AWS. Genetic engineered molecular imaging probes for applications in cell therapy: emphasis on MRI approach. *Am J Nucl Med Mol Imaging* 2016, 6:234–261.
  25. Youn HCJ. Reporter gene imaging. *Am J Roentgenol* 2013, 201:W206–W214.
  26. Dash R, Chung J, Ikeno F, Hahn-Windgassen A, Matsuura Y, Bennett MV, Lyons JK, Teramoto T, Robbins RC, McConnell MV, et al. Dual manganese-enhanced and delayed gadolinium-enhanced MRI detects myocardial border zone injury in a pig ischemia-reperfusion model. *Circ Cardiovasc Imaging* 2011, 4:574–582.
  27. Mezer A, Yeatman JD, Stikov N, Kay KN, Cho NJ, Dougherty RF, Perry ML, Parvizi J, Hua le H, Butts-Pauly K, et al. Quantifying the local tissue volume and composition in individual brains with magnetic resonance imaging. *Nat Med* 2013, 19:1667–1672.
  28. Wedeen VJ, Hagmann P, Tseng WY, Reese TG, Weisskoff RM. Mapping complex tissue architecture with diffusion spectrum magnetic resonance imaging. *Magn Reson Med* 2005, 54:1377–1386.
  29. Sosnovik DE, Wang R, Dai G, Wang T, Aikawa E, Novikov M, Rosenzweig A, Gilbert RJ, Wedeen VJ. Diffusion spectrum MRI tractography reveals the presence of a complex network of residual myofibers in infarcted myocardium. *Circ Cardiovasc Imaging* 2009, 2:206–212.
  30. Zhou J, Payen JF, Wilson DA, Traystman RJ, van Zijl PC. Using the amide proton signals of intracellular proteins and peptides to detect pH effects in MRI. *Nat Med* 2003, 9:1085–1090.
  31. Bar-Shir A, Liu G, Chan KW, Oskolkov N, Song X, Yadav NN, Walczak P, McMahon MT, van Zijl PC, Bulte JW, et al. Human protamine-1 as an MRI reporter gene based on chemical exchange. *ACS Chem Biol* 2014, 9:134–138.
  32. Ward KM, Aletras AH, Balaban RS. A new class of contrast agents for MRI based on proton chemical exchange dependent saturation transfer (CEST). *J Magn Reson* 2000, 143:79–87.
  33. van Zijl PC, Yadav NN. Chemical exchange saturation transfer (CEST): what is in a name and what isn't? *Magn Reson Med* 2011, 65:927–948.
  34. Chan KW, Liu G, Song X, Kim H, Yu T, Arifin DR, Gilad AA, Hanes J, Walczak P, van Zijl PC, et al. MRI-detectable pH nanosensors incorporated into hydrogels for in vivo sensing of transplanted-cell viability. *Nat Mater* 2013, 12:268–275.
  35. Nelson SJ, Ozhinsky E, Li Y, Park I, Crane J. Strategies for rapid in vivo  $^1\text{H}$  and hyperpolarized  $^{13}\text{C}$  MR spectroscopic imaging. *J Magn Reson* 2013, 229:187–197.
  36. Zhu H, Barker PB. MR spectroscopy and spectroscopic imaging of the brain. *Methods Mol Biol* 2011, 711:203–226.
  37. Haris M, Singh A, Cai K, Kogan F, McGarvey J, Debrosse C, Zsido GA, Witschey WR, Koomalsingh K, Pilla JJ, et al. A technique for in vivo mapping of myocardial creatine kinase metabolism. *Nat Med* 2014, 20:209–214.



38. Naresh NK, Chen X, Roy RJ, Antkowiak PF, Annex BH, Epstein FH. Accelerated dual-contrast first-pass perfusion MRI of the mouse heart: development and application to diet-induced obese mice. *Magn Reson Med* 2015, 73:1237–1245.
39. Robbers LF, Nijveldt R, Beek AM, Hirsch A, van der Laan AM, Delewi R, van der Vleuten PA, Tio RA, Tijssen JG, Hofman MB, et al. Cell therapy in reperfused acute myocardial infarction does not improve the recovery of perfusion in the infarcted myocardium: a cardiac MR imaging study. *Radiology* 2014, 272:113–122.
40. Kerwin WS, Naumova A, Storb R, Tapscott SJ, Wang Z. Mapping contrast agent uptake and retention in MRI studies of myocardial perfusion: case control study of dogs with Duchenne muscular dystrophy. *Int J Cardiovasc Imaging* 2013, 29:819–826.
41. Kerwin WS, Zhao X, Yuan C, Hatsukami TS, Maravilla KR, Underhill HR, Zhao X. Contrast-enhanced MRI of carotid atherosclerosis: dependence on contrast agent. *J Magn Reson Imaging* 2009, 30:35–40.
42. Henningsson M, Greil GF, Burch M, Hussain T, Taylor AM, Muthurangu V, Botnar RM, Dedieu N. Coronary magnetic resonance angiography in heterotopic heart transplant recipient. *Circulation* 2014, 129:1453–1455.
43. Stadlbauer A, Zimmermann M, Heinz G, Oberndorfer S, Doerfler A, Buchfelder M, Rossler K. Magnetic resonance imaging biomarkers for clinical routine assessment of microvascular architecture in glioma. *J Cereb Blood Flow Metab* 2017, 37:632–643.
44. Vande Velde G, Baekelandt V, Dresselaers T, Himmelreich U. Magnetic resonance imaging and spectroscopy methods for molecular imaging. *Q J Nucl Med Mol Imaging* 2009, 53:565–585.
45. Yang C, Tian R, Liu T, Liu G. MRI reporter genes for noninvasive molecular imaging. *Molecules* 2016, 21:580.
46. Vandsburger MH, Radoul M, Cohen B, Neeman M. MRI reporter genes: application to imaging of cell survival, proliferation, migration, and differentiation. *NMR Biomed* 2013, 26:872–884.
47. Vandsburger M. Cardiac cell tracking with MRI reporter genes: welcoming a new field. *Curr Cardiovasc Imaging Rep* 2014, 7:9250.
48. Vande Velde G, Raman Rangarajan J, Vreys R, Guglielmetti C, Dresselaers T, Verhoye M, Van der Linden A, Debyser Z, Baekelandt V, Maes F, et al. Quantitative evaluation of MRI-based tracking of ferritin-labeled endogenous neural stem cell progeny in rodent brain. *Neuroimage* 2012, 62:367–380.
49. Gu ECW, Gu J, Burridge P, Wu JC. Molecular imaging of stem cells: tracking survival, biodistribution, tumorigenicity, and immunogenicity. *Theranostics* 2012, 2:335–345.
50. Nguyen PKLF, Wang Y, Wu JC. Imaging: guiding the clinical translation of cardiac stem cell therapy. *Circ Res* 2011, 109:962–979.
51. Cohen B, Dafni H, Meir G, Harmelin A, Neeman M. Ferritin as an endogenous MRI reporter for noninvasive imaging of gene expression in C6 glioma tumors. *Neoplasia* 2005, 7:109–117.
52. Genove G, DeMarco U, Xu H, Goins WF, Ahrens ET. A new transgene reporter for in vivo magnetic resonance imaging. *Nat Med* 2005, 11:450–454.
53. Naumova AV, Reinecke H, Yarnykh V, Deem J, Yuan C, Murry CE. Ferritin overexpression for noninvasive magnetic resonance imaging-based tracking of stem cells transplanted into the heart. *Mol Imaging* 2010, 9:201–210.
54. Vande Velde G, Rangarajan JR, Toelen J, Dresselaers T, Ibrahim A, Krylychkina O, Vreys R, Van der Linden A, Maes F, Debyser Z, et al. Evaluation of the specificity and sensitivity of ferritin as an MRI reporter gene in the mouse brain using lentiviral and adeno-associated viral vectors. *Gene Ther* 2011, 18:594–605.
55. Koretsky A, Lin Y, Schorle H, Jaenisch R. Genetic control of MRI contrast by expression of the transferrin receptor. In: *Proceedings of the Fourth Meeting of the International Society for Magnetic Resonance in Medicine, New York, 27 April – 03 May, 1996*.
56. Moore A, Josephson L, Bhorade RM, Basilion JP, Weissleder R. Human transferrin receptor gene as a marker gene for MR imaging. *Radiology* 2001, 221:244–250.
57. Deans AE, Wadghiri YZ, Bernas LM, Yu X, Rutt BK, Turnbull DH. Cellular MRI contrast via coexpression of transferrin receptor and ferritin. *Magn Reson Med* 2006, 56:51–59.
58. Bartelle BB, Szulc KU, Suero-Abreu GA, Rodriguez JJ, Turnbull DH. Divalent metal transporter, DMT1: a novel MRI reporter protein. *Magn Reson Med* 2013, 70:842–850.
59. Chen TT, Li L, Chung DH, Allen CD, Torti SV, Torti FM, Cyster JG, Chen CY, Brodsky FM, Niemi EC, et al. TIM-2 is expressed on B cells and in liver and kidney and is a receptor for H-ferritin endocytosis. *J Exp Med* 2005, 202:955–965.
60. Todorich B, Zhang X, Slagle-Webb B, Seaman WE, Connor JR. Tim-2 is the receptor for H-ferritin on oligodendrocytes. *J Neurochem* 2008, 107:1495–1505.
61. Patrick PS, Rodrigues TB, Kettunen MI, Lyons SK, Neves AA, Brindle KM. Development of Tim2 as a reporter gene for MRI. *Magn Reson Med* 2016, 75:1697–1707.
62. Shapiro MGRR, Sperling LJ, Sun G, Sun J, Pines A, Schaffer DV, Bajaj VS. Genetically encoded reporters for hyperpolarized xenon magnetic resonance imaging. *Nat Chem* 2014, 6:629–634.

63. Walczak P, Kedziorek DA, Gilad AA, Barnett BP, Bulte JW. Applicability and limitations of MR tracking of neural stem cells with asymmetric cell division and rapid turnover: the case of the shiverer dysmyelinated mouse brain. *Magn Reson Med* 2007, 58:261–269.
64. Arbab AS, Bashaw LA, Miller BR, Jordan EK, Lewis BK, Kalish H, Frank JA. Characterization of biophysical and metabolic properties of cells labeled with superparamagnetic iron oxide nanoparticles and transfection agent for cellular MR imaging. *Radiology* 2003, 229:838–846.
65. Thu MS, Bryant LH, Coppola T, Jordan EK, Budde MD, Lewis BK, Chaudhry A, Ren J, Varma NR, Arbab AS, et al. Self-assembling nanocomplexes by combining ferumoxytol, heparin and protamine for cell tracking by magnetic resonance imaging. *Nat Med* 2012, 18:463–467.
66. Amsalem Y, Mardor Y, Feinberg MS, Landa N, Miller L, Daniels D, Ocherashvilli A, Holbova R, Yosef O, Barbash IM, et al. Iron-oxide labeling and outcome of transplanted mesenchymal stem cells in the infarcted myocardium. *Circulation* 2007, 116:I38–I45.
67. Terrovitis J, Stuber M, Youssef A, Preece S, Leppo M, Kizana E, Schar M, Gerstenblith G, Weiss RG, Marban E, et al. Magnetic resonance imaging overestimates ferumoxide-labeled stem cell survival after transplantation in the heart. *Circulation* 2008, 117:1555–1562.
68. Naumova AV, Balu N, Yarnykh VL, Reinecke H, Murry CE, Yuan C. Magnetic resonance imaging tracking of graft survival in the infarcted heart: iron oxide particles versus ferritin overexpression approach. *J Cardiovasc Pharmacol Ther* 2014, 19:358–367.
69. Schafer R, Kehlbach R, Muller M, Bantleon R, Kluba T, Ayturan M, Siegel G, Wolburg H, Northoff H, Dietz K, et al. Labeling of human mesenchymal stromal cells with superparamagnetic iron oxide leads to a decrease in migration capacity and colony formation ability. *Cytotherapy* 2009, 11:68–78.
70. Kostura L, Kraitchman DL, Mackay AM, Pittenger MF, Bulte JW. Feridex labeling of mesenchymal stem cells inhibits chondrogenesis but not adipogenesis or osteogenesis. *NMR Biomed* 2004, 17:513–517.
71. Chung J, Kee K, Barral JK, Dash R, Kosuge H, Wang X, Weissman I, Robbins RC, Nishimura D, Quertermous T, et al. In vivo molecular MRI of cell survival and teratoma formation following embryonic stem cell transplantation into the injured murine myocardium. *Magn Reson Med* 2011, 66:1374–1381.
72. Louie AY, Huber MM, Ahrens ET, Rothbacher U, Moats R, Jacobs RE, Fraser SE, Meade TJ. In vivo visualization of gene expression using magnetic resonance imaging. *Nat Biotechnol* 2000, 18:321–325.
73. Bulte JW. In vivo MRI cell tracking: clinical studies. *AJR Am J Roentgenol* 2009, 193:314–325.
74. Zhu J, Zhou L, XingWu F. Tracking neural stem cells in patients with brain trauma. *N Engl J Med* 2006, 355:2376–2378.
75. Liu L, Ye Q, Wu Y, Hsieh WY, Chen CL, Shen HH, Wang SJ, Zhang H, Hitchens TK, Ho C. Tracking T-cells in vivo with a new nano-sized MRI contrast agent. *Nanomedicine* 2012, 8:1345–1354.
76. Bauer LM, Situ SF, Griswold MA, Samia AC. Magnetic particle imaging tracers: state-of-the-art and future directions. *J Phys Chem Lett* 2015, 6:2509–2517.
77. Zheng B, von See MP, Yu E, Gunel B, Lu K, Vazin T, Schaffer DV, Goodwill PW, Conolly SM. Quantitative magnetic particle imaging monitors the transplantation, biodistribution, and clearance of stem cells in vivo. *Theranostics* 2016, 6:291–301.
78. Bulte JW, Walczak P, Janowski M, Krishnan KM, Arami H, Halkola A, Gleich B, Rahmer J. Quantitative “hot spot” imaging of transplanted stem cells using superparamagnetic tracers and magnetic particle imaging (MPI). *Tomography* 2015, 1:91–97.
79. Zheng B, Vazin T, Goodwill PW, Conway A, Verma A, Saritas EU, Schaffer D, Conolly SM. Magnetic particle imaging tracks the long-term fate of in vivo neural cell implants with high image contrast. *Sci Rep* 2015, 5:14055.
80. Naumova AV, Yarnykh VL, Balu N, Reinecke H, Murry CE, Yuan C. Quantification of MRI signal of transgenic grafts overexpressing ferritin in murine myocardial infarcts. *NMR Biomed* 2012, 25:1187–1195.
81. Liu J, Cheng EC, Long RC, Yang SH, Wang L, Cheng PH, Yang J, Wu D, Mao H, Chan AW. Noninvasive monitoring of embryonic stem cells in vivo with MRI transgene reporter. *Tissue Eng Part C Methods* 2009, 15:739–747.
82. Naumova AV, Yarnykh V, Balu N, Reinecke H, Murry CE, Yuan C. Improved identification of ferritin-tagged grafts in mouse heart at higher magnetic field strength. In: *Proceedings of the ISMRM Melbourne, Australia*, 5–11 May, 2012.
83. Shi H, Bencze KZ, Stemmler TL, Philpott CC. A cytosolic iron chaperone that delivers iron to ferritin. *Science* 2008, 320:1207–1210.
84. Kilcoyne SH, Cywinski R. Ferritin: a model superparamagnet. *J Magn Magn Mater* 1995, 140:1466–1467.
85. Brooks RA, Vymazal J, Goldfarb RB, Bulte JWM, Aisen P. Relaxometry and magnetometry of ferritin. *Magn Reson Med* 1998, 40:227–235.
86. Pantopoulos K, Porwal SK, Tartakoff A, Devireddy L. Mechanisms of mammalian iron homeostasis. *Biochemistry* 2012, 51:5705–5724.

87. Wang J, Pantopoulos K. Regulation of cellular iron metabolism. *Biochem J* 2011, 434:365–381.
88. Hentze MW, Muckenthaler MU, Galy B, Camaschella C. Two to tango: regulation of mammalian iron metabolism. *Cell* 2010, 142:24–38.
89. Ponka P, Lok CN. The transferrin receptor: role in health and disease. *Int J Biochem Cell Biol* 1999, 31:1111–1137.
90. Enns CA, Shindelman JE, Tonik SE, Sussman HH. Radioimmunochemical measurement of the transferrin receptor in human trophoblast and reticulocyte membranes with a specific anti-receptor antibody. *Proc Natl Acad Sci USA* 1981, 78:4222–4225.
91. Davies M, Parry JE, Sutcliffe RG. Examination of different preparations of human placental plasma membrane for the binding of insulin, transferrin and immunoglobulins. *J Reprod Fertil* 1981, 63:315–324.
92. Gatter KC, Brown G, Trowbridge IS, Woolston RE, Mason DY. Transferrin receptors in human tissues: their distribution and possible clinical relevance. *J Clin Pathol* 1983, 36:539–545.
93. Wada HG, Hass PE, Sussman HH. Transferrin receptor in human placental brush border membranes. Studies on the binding of transferrin to placental membrane vesicles and the identification of a placental brush border glycoprotein with high affinity for transferrin. *J Biol Chem* 1979, 254:12629–12635.
94. Thorstensen K, Romslo I. The role of transferrin in the mechanism of cellular iron uptake. *Biochem J* 1990, 271:1–9.
95. Anderson GJ, Vulpe CD. Mammalian iron transport. *Cell Mol Life Sci* 2009, 66:3241–3261.
96. Aisen P. Entry of iron into cells: a new role for the transferrin receptor in modulating iron release from transferrin. *Ann Neurol* 1992, 32(Suppl S1):S62–S68.
97. Levy JE, Jin O, Fujiwara Y, Kuo F, Andrews NC. Transferrin receptor is necessary for development of erythrocytes and the nervous system. *Nat Genet* 1999, 21:396–399.
98. Meldrum F, Heywood B, Mann S. Magnetoferritin: in vitro synthesis of a novel magnetic protein. *Science* 1992, 257:522–523.
99. Harrison PM, Arosio P. Ferritins: molecular properties, iron storage function and cellular regulation. *Biochim Biophys Acta Bioenerg* 1996, 1275:161–203.
100. Treffry A, Zhao Z, Quail MA, Guest JR, Harrison PM. Dinuclear center of ferritin: studies of iron binding and oxidation show differences in the two iron sites. *Biochemistry* 1997, 36:432–441.
101. Ford GC, Harrison PM, Rice DW, Smith JMA, Treffry A, White JL, Yariv J. Ferritin: design and formation of an iron-storage molecule. *Philos Trans R Soc Lond B Biol Sci* 1984, 304:551–565.
102. Matsumoto Y, Chen R, Anikeeva P, Jasanoff A. Engineering intracellular biomineralization and biosensing by a magnetic protein. *Nat Commun* 2015, 6:8721.
103. Zhao G, Bou-Abdallah F, Arosio P, Levi S, Januschandler C, Chasteen ND. Multiple pathways for mineral core formation in mammalian apoferritin. The role of hydrogen peroxide. *Biochemistry* 2003, 42:3142–3150.
104. Frankel RB, Papaefthymiou GC, Watt GD. Variation of superparamagnetic properties with iron loading in mammalian ferritin. *Hyperfine Interact* 1991, 66:71–82.
105. Valko M, Morris H, Cronin MT. Metals, toxicity and oxidative stress. *Curr Med Chem* 2005, 12:1161–1208.
106. Crichton RR, Wilmet S, Leggsyter R, Ward RJ. Molecular and cellular mechanisms of iron homeostasis and toxicity in mammalian cells. *J Inorg Biochem* 2002, 91:9–18.
107. Arosio P, Levi S. Ferritin, iron homeostasis, and oxidative damage. *Free Radic Biol Med* 2002, 33:457–463.
108. Munro HN, Linder MC. Ferritin: structure, biosynthesis, and role in iron metabolism. *Physiol Rev* 1978, 58:317–396.
109. Theil EC. Ferritin: structure, gene regulation, and cellular function in animals, plants, and microorganisms. *Annu Rev Biochem* 1987, 56:289–315.
110. Ferreira C, Bucchini D, Martin ME, Levi S, Arosio P, Grandchamp B, Beaumont C. Early embryonic lethality of H ferritin gene deletion in mice. *J Biol Chem* 2000, 275:3021–3024.
111. Li JY, Paragas N, Ned RM, Qiu A, Viltard M, Leete T, Drexler IR, Chen X, Sanna-Cherchi S, Mohammed F, et al. Scara5 is a ferritin receptor mediating non-transferrin iron delivery. *Dev Cell* 2009, 16:35–46.
112. Shayeghi M, Latunde-Dada GO, Oakhill JS, Laftah AH, Takeuchi K, Halliday N, Khan Y, Warley A, McCann FE, Hider RC, et al. Identification of an intestinal heme transporter. *Cell* 2005, 122:789–801.
113. Rajagopal A, Rao AU, Amigo J, Tian M, Upadhyay SK, Hall C, Uhm S, Mathew MK, Fleming MD, Paw BH, et al. Haem homeostasis is regulated by the conserved and concerted functions of HRG-1 proteins. *Nature* 2008, 453:1127–1131.
114. Levi S, Corsi B, Bosisio M, Invernizzi R, Volz A, Sanford D, Arosio P, Drysdale J. A human mitochondrial ferritin encoded by an intronless gene. *J Biol Chem* 2001, 276:24437–24440.
115. Santambrogio P, Biasiotto G, Sanvito F, Olivieri S, Arosio P, Levi S. Mitochondrial ferritin expression in adult mouse tissues. *J Histochem Cytochem* 2007, 55:1129–1137.

116. Nie G, Sheftel AD, Kim SF, Ponka P. Overexpression of mitochondrial ferritin causes cytosolic iron depletion and changes cellular iron homeostasis. *Blood* 2005, 105:2161–2167.
117. Corsi B, Cozzi A, Arosio P, Drysdale J, Santambrogio P, Campanella A, Biasiotto G, Albertini A, Levi S. Human mitochondrial ferritin expressed in HeLa cells incorporates iron and affects cellular iron metabolism. *J Biol Chem* 2002, 277:22430–22437.
118. Wish JB. Assessing iron status: beyond serum ferritin and transferrin saturation. *Clin J Am Soc Nephrol* 2006, 1:54–58.
119. De Domenico I, Ward DM, Kaplan J. Specific iron chelators determine the route of ferritin degradation. *Blood* 2009, 114:4546–4551.
120. Ofer S, Fibach E, Kessel M, Bauminger E, Cohen S, Eikelboom J, Rachmilewitz E. Iron incorporation into ferritin and hemoglobin during differentiation of murine erythroleukemia cells. *Blood* 1981, 58:255–262.
121. Weir MP, Sharp GA, Peters TJ. Electron microscopic studies of human haemosiderin and ferritin. *J Clin Pathol* 1985, 38:915–918.
122. Koorts AM, Viljoen M. Ferritin and ferritin isoforms II: protection against uncontrolled cellular proliferation, oxidative damage and inflammatory processes. *Arch Physiol Biochem* 2007, 113:55–64.
123. Koorts AM, Viljoen M. Ferritin and ferritin isoforms I: structure–function relationships, synthesis, degradation and secretion. *Arch Physiol Biochem* 2007, 113:30–54.
124. Schenck JF, Zimmerman EA. High-field magnetic resonance imaging of brain iron: birth of a biomarker? *NMR Biomed* 2004, 17:433–445.
125. Berg D, Youdim MB. Role of iron in neurodegenerative disorders. *Top Magn Reson Imaging* 2006, 17:5–17.
126. Ropele S, Kilsdonk ID, Wattjes MP, Langkammer C, WlD G, Frederiksen JL, Larsson HB, Yiannakas M, Wheeler-Kingshott CA, Enzinger C, et al. Determinants of iron accumulation in deep grey matter of multiple sclerosis patients. *Mult Scler J* 2014, 20:1692–1698.
127. Khalil M, Langkammer C, Pichler A, Pinter D, Gatteringer T, Bachmaier G, Ropele S, Fuchs S, Enzinger C, Fazekas F. Dynamics of brain iron levels in multiple sclerosis: a longitudinal 3T MRI study. *Neurology* 2015, 84:2396–2402.
128. Ghadery C, Pirpamer L, Hofer E, Langkammer C, Petrovic K, Loitfelder M, Schwingenschuh P, Seiler S, Duering M, Jouvent E, et al. R2\* mapping for brain iron: associations with cognition in normal aging. *Neurobiol Aging* 2015, 36:925–932.
129. Aisen P. Transferrin, the transferrin receptor, and the uptake of iron by cells. *Met Ions Biol Syst* 1998, 35:585–631.
130. Huebers HA, Finch CA. The physiology of transferrin and transferrin receptors. *Physiol Rev* 1987, 67:520–582.
131. Bridges KR, Cudkowicz A. Effect of iron chelators on the transferrin receptor in K562 cells. *J Biol Chem* 1984, 259:12970–12977.
132. Rao KK, Shapiro D, Mattia E, Bridges K, Klausner R. Effects of alterations in cellular iron on biosynthesis of the transferrin receptor in K562 cells. *Mol Cell Biol* 1985, 5:595–600.
133. Ward JH, Jordan I, Kushner JP, Kaplan J. Heme regulation of HeLa cell transferrin receptor number. *J Biol Chem* 1984, 259:13235–13240.
134. Moore A, Basilion JP, Chiocca EA, Weissleder R. Measuring transferrin receptor gene expression by NMR imaging. *Biochim Biophys Acta* 1998, 1402:239–249.
135. Sotak CH, Sharer K, Koretsky AP. Manganese cell labeling of murine hepatocytes using manganese(III)-transferrin. *Contrast Media Mol Imaging* 2008, 3:95–105.
136. Feng Y, Liu Q, Zhu J, Xie F, Li L. Efficiency of ferritin as an MRI reporter gene in NPC cells is enhanced by iron supplementation. *J Biomed Biotechnol* 2012, 2012:434878.
137. Kim HS, Cho HR, Choi SH, Woo JS, Moon WK. In vivo imaging of tumor transduced with bimodal lentiviral vector encoding human ferritin and green fluorescent protein on a 1.5T clinical magnetic resonance scanner. *Cancer Res* 2010, 70:7315–7324.
138. Ono K, Fuma K, Tabata K, Sawada M. Ferritin reporter used for gene expression imaging by magnetic resonance. *Biochem Biophys Res Commun* 2009, 388:589–594.
139. Cohen B, Ziv K, Plaks V, Israely T, Kalchenko V, Harmelin A, Benjamin LE, Neeman M. MRI detection of transcriptional regulation of gene expression in transgenic mice. *Nat Med* 2007, 13:498–503.
140. Ziv K, Meir G, Harmelin A, Shimoni E, Klein E, Neeman M. Ferritin as a reporter gene for MRI: chronic liver over expression of H-ferritin during dietary iron supplementation and aging. *NMR Biomed* 2010, 23:523–531.
141. Uchida M, Terashima M, Cunningham CH, Suzuki Y, Willits DA, Willis AF, Yang PC, Tsao PS, McConnell MV, Young MJ, et al. A human ferritin iron oxide nano-composite magnetic resonance contrast agent. *Magn Reson Med* 2008, 60:1073–1081.
142. Terashima M, Uchida M, Kosuge H, Tsao PS, Young MJ, Conolly SM, Douglas T, McConnell MV. Human ferritin cages for imaging vascular macrophages. *Biomaterials* 2011, 32:1430–1437.

143. Bulte JWM, Douglas T, Mann S, Frankel RB, Moskowicz BM, Brooks RA, Baumbarner CD, Vymazal J, Frank JA. Magnetoferritin: biomineralization as a novel molecular approach in the design of iron-oxide-based magnetic resonance contrast agents. *Invest Radiol* 1994, 29:S214–S216.
144. Bulte JWM, Douglas T, Mann S, Frankel RB, Moskowicz BM, Brooks RA, Baumgarner CD, Vymazal J, Strub M-P, Frank JA. Magnetoferritin: characterization of a novel superparamagnetic MR contrast agent. *J Magn Reson Imaging* 1994, 4:497–505.
145. Bulte JWM, Douglas T, Mann S, Vymazal J, Laughlin PG, Frank JA. Initial assessment of magnetoferritin biokinetics and proton relaxation enhancement in rats. *Acad Radiol* 1995, 2:871–878.
146. Iordanova B, Hitchens TK, Robison CS, Ahrens ET. Engineered mitochondrial ferritin as a magnetic resonance imaging reporter in mouse olfactory epithelium. *PLoS One* 2013, 8:e72720.
147. Iordanova B, Robison CS, Ahrens ET. Design and characterization of a chimeric ferritin with enhanced iron loading and transverse NMR relaxation rate. *J Biol Inorg Chem* 2010, 15:957–965.
148. Aung W, Hasegawa S, Koshikawa-Yano M, Obata T, Ikehira H, Furukawa T, Aoki I, Saga T. Visualization of in vivo electroporation-mediated transgene expression in experimental tumors by optical and magnetic resonance imaging. *Gene Ther* 2009, 16:830–839.
149. Blakemore R. Magnetotactic bacteria. *Science* 1975, 190:377–379.
150. Bazylinski DA, Frankel RB. Magnetosome formation in prokaryotes. *Nat Rev Microbiol* 2004, 2:217–230.
151. Goldhawk DE, Rohani R, Sengupta A, Gelman N, Prato FS. Using the magnetosome to model effective gene-based contrast for magnetic resonance imaging. *WIREs Nanomed Nanobiotechnol* 2012, 4:378–388.
152. Nakamura C, Kikuchi T, Burgess JG, Matsunaga T. Iron-regulated expression and membrane localization of the magA protein in *Magnetospirillum* sp. strain AMB-1. *J Biochem* 1995, 118:23–27.
153. Murat D, Quinlan A, Vali H, Komeili A. Comprehensive genetic dissection of the magnetosome gene island reveals the step-wise assembly of a prokaryotic organelle. *Proc Natl Acad Sci USA* 2010, 107:5593–5598.
154. Uebe R, Henn V, Schuler D. The MagA protein of *Magnetospirilla* is not involved in bacterial magnetite biomineralization. *J Bacteriol* 2012, 194:1018–1023.
155. Zurkiya O, Chan AW, Hu X. MagA is sufficient for producing magnetic nanoparticles in mammalian cells, making it an MRI reporter. *Magn Reson Med* 2008, 59:1225–1231.
156. Goldhawk DE, Lemaire C, McCreary CR, McGirr R, Dhanvantari S, Thompson RT, Figueredo R, Koropatnick J, Foster P, Prato FS. Magnetic resonance imaging of cells overexpressing MagA, an endogenous contrast agent for live cell imaging. *Mol Imaging* 2009, 8:129–139.
157. Nakamura C, Burgess JG, Sode K, Matsunaga T. An iron-regulated gene, magA, encoding an iron transport protein of *Magnetospirillum* sp. strain AMB-1. *J Biol Chem* 1995, 270:28392–28396.
158. Cho IK, Moran SP, Paudyal R, Piotrowska-Nitsche K, Cheng P-H, Zhang X, Mao H, Chan AWS. Longitudinal monitoring of stem cell grafts in vivo using magnetic resonance imaging with inducible magA as a genetic reporter. *Theranostics* 2014, 4:972–989.
159. Guan X, Jiang X, Yang C, Tian X, Li L. The MRI marker gene MagA attenuates the oxidative damage induced by iron overload in transgenic mice. *Nanotoxicology* 2016, 10:531–541.
160. Sengupta A, Quiaoit K, Thompson RT, Prato FS, Gelman N, Goldhawk DE. Biophysical features of MagA expression in mammalian cells: implications for MRI contrast. *Front Microbiol* 2014, 5:29.
161. Zhang XY, Robledo BN, Harris SS, Hu XP. A bacterial gene, mms6, as a new reporter gene for magnetic resonance imaging of mammalian cells. *Mol Imaging* 2014, 13. doi: 10.2310/7290.2014.00046.
162. Radoul M, Lewin L, Cohen B, Oren R, Popov S, Davidov G, Vandsburger MH, Harmelin A, Bitton R, Greneche J-M, et al. Genetic manipulation of iron biomineralization enhances MR relaxivity in a ferritin-M6A chimeric complex. *Sci Rep* 2016, 6:26550.
163. Han J, Seaman WE, Di X, Wang W, Willingham M, Torti FM, Torti SV. Iron uptake mediated by binding of H-ferritin to the TIM-2 receptor in mouse cells. *PLoS One* 2011, 6:e23800.
164. Maguire CA, Ramirez SH, Merkel SF, Sena-Esteves M, Breakefield XO. Gene therapy for the nervous system: challenges and new strategies. *Neurotherapeutics* 2014, 11:817–839.
165. Schmidt F, Grimm D. CRISPR genome engineering and viral gene delivery: a case of mutual attraction. *Biotechnol J* 2015, 10:258–272.
166. Grimm D, Kern A, Rittner K, Kleinschmidt JA. Novel tools for production and purification of recombinant adenoassociated virus vectors. *Hum Gene Ther* 1998, 9:2745–2760.
167. Shearer RF, Saunders DN. Experimental design for stable genetic manipulation in mammalian cell lines: lentivirus and alternatives. *Genes Cells* 2015, 20:1–10.
168. Chatterjee S, De A. Applications of lentiviral vectors in molecular imaging. *Front Biosci (Landmark Ed)* 2014, 19:835–853.

169. Šimčíková M, Prather KLJ, Prazeres DMF, Monteiro GA. Towards effective non-viral gene delivery vector. *Biotechnol Genet Eng Rev* 2015, 31:82–107.
170. Reynolds BA, Weiss S. Generation of neurons and astrocytes from isolated cells of the adult mammalian central nervous system. *Science* 1992, 255:1707–1710.
171. Eriksson PS, Perfilieva E, Bjork-Eriksson T, Alborn AM, Nordborg C, Peterson DA, Gage FH. Neurogenesis in the adult human hippocampus. *Nat Med* 1998, 4:1313–1317.
172. Vande Velde G, Couillard-Després S, Aigner L, Himmelreich U, van der Linden A. In situ labeling and imaging of endogenous neural stem cell proliferation and migration. *WIREs Nanomed Nanobiotechnol* 2012, 4:663–679.
173. Vreys R, Vande Velde G, Krylychkina O, Vellema M, Verhoye M, Timmermans JP, Baekelandt V, Van der Linden A. MRI visualization of endogenous neural progenitor cell migration along the RMS in the adult mouse brain: validation of various MPIO labeling strategies. *Neuroimage* 2010, 49:2094–2103.
174. Sumner JP, Shapiro EM, Maric D, Conroy R, Koretsky AP. In vivo labeling of adult neural progenitors for MRI with micron sized particles of iron oxide: quantification of labeled cell phenotype. *Neuroimage* 2009, 44:671–678.
175. Panizzo RA, Kyrtatos PG, Price AN, Gadian DG, Ferretti P, Lythgoe MF. In vivo magnetic resonance imaging of endogenous neuroblasts labelled with a ferumoxide-polycation complex. *Neuroimage* 2009, 44:1239–1246.
176. Shapiro EM, Gonzalez-Perez O, Manuel Garcia-Verdugo J, Alvarez-Buylla A, Koretsky AP. Magnetic resonance imaging of the migration of neuronal precursors generated in the adult rodent brain. *Neuroimage* 2006, 32:1150–1157.
177. Yang J, Liu J, Niu G, Chan KC, Wang R, Liu Y, Wu EX. In vivo MRI of endogenous stem/progenitor cell migration from subventricular zone in normal and injured developing brains. *Neuroimage* 2009, 48:319–328.
178. Granot D, Scheinost D, Markakis EA, Papademetris X, Shapiro EM. Serial monitoring of endogenous neuroblast migration by cellular MRI. *Neuroimage* 2011, 57:817–824.
179. Iordanova B, Ahrens ET. In vivo magnetic resonance imaging of ferritin-based reporter visualizes native neuroblast migration. *Neuroimage* 2012, 59:1004–1012.
180. Elhami E, Dietz B, Xiang B, Deng J, Wang F, Chi C, Goertzen AL, Mzengeza S, Freed D, Arora RC, et al. Assessment of three techniques for delivering stem cells to the heart using PET and MR imaging. *EJNMMI Res* 2013, 3:72.
181. Li Z, Suzuki Y, Huang M, Cao F, Xie X, Connolly AJ, Yang PC, Wu JC. Comparison of reporter gene and iron particle labeling for tracking fate of human embryonic stem cells and differentiated endothelial cells in living subjects. *Stem Cells* 2008, 26:864–873.
182. Campan M, Lionetti V, Aquaro GD, Forini F, Matteucci M, Vannucci L, Chiappesi F, Di Cristofano C, Faggioni M, Maioli M, et al. Ferritin as a reporter gene for in vivo tracking of stem cells by 1.5-T cardiac MRI in a rat model of myocardial infarction. *Am J Physiol Heart Circ Physiol* 2011, 300:H2238–H2250.
183. Weissleder R, Pittet MJ. Imaging in the era of molecular oncology. *Nature* 2008, 452:580–589.
184. Li C, Penet MF, Winnard P Jr, Artemov D, Bhujwala ZM. Image-guided enzyme/prodrug cancer therapy. *Clin Cancer Res* 2008, 14:515–522.
185. Li C, Penet MF, Wildes F, Takagi T, Chen Z, Winnard PT, Artemov D, Bhujwala ZM. Nanoplex delivery of siRNA and prodrug enzyme for multimodality image-guided molecular pathway targeted cancer therapy. *ACS Nano* 2010, 4:6707–6716.
186. Weissleder R, Moore A, Mahmood U, Borhade R, Benveniste H, Chioocca EA, Basilion JP. In vivo magnetic resonance imaging of transgene expression. *Nat Med* 2000, 6:351–355.
187. Jensen JH, Chandra R. Theory of nonexponential NMR signal decay in liver with iron overload or superparamagnetic iron oxide particles. *Magn Reson Med* 2002, 47:1131–1138.
188. Wu EX, Kim D, Tosti CL, Tang H, Jensen JH, Cheung JS, Feng L, Au WY, Ha SY, Sheth SS, et al. Magnetic resonance assessment of iron overload by separate measurement of tissue ferritin and hemosiderin iron. *Ann N Y Acad Sci* 2010, 1202:115–122.
189. Jensen JH, Tang H, Tosti CL, Swaminathan SV, Nunez A, Hultman K, Szulc KU, Wu EX, Kim D, Sheth S, et al. Separate MRI quantification of dispersed (ferritin-like) and aggregated (hemosiderin-like) storage iron. *Magn Reson Med* 2010, 63:1201–1209.
190. Patil S, Jirak D, Saudek F, Hajek M, Scheffler K. Positive contrast visualization of SPIO-labeled pancreatic islets using echo-dephased steady-state free precession. *Eur Radiol* 2011, 21:214–220.
191. Cunningham CH, Arai T, Yang PC, McConnell MV, Pauly JM, Conolly SM. Positive contrast magnetic resonance imaging of cells labeled with magnetic nanoparticles. *Magn Reson Med* 2005, 53:999–1005.
192. Mills PH, Ahrens ET. Enhanced positive-contrast visualization of paramagnetic contrast agents using phase images. *Magn Reson Med* 2009, 62:1349–1355.
193. Dahnke H, Liu W, Herzka D, Frank JA, Schaeffter T. Susceptibility gradient mapping (SGM): a new

- postprocessing method for positive contrast generation applied to superparamagnetic iron oxide particle (SPIO)-labeled cells. *Magn Reson Med* 2008, 60:595–603.
194. Shapiro EM, Sharer K, Skrtic S, Koretsky AP. In vivo detection of single cells by MRI. *Magn Reson Med* 2006, 55:242–249.
  195. Bennett KM, Shapiro EM, Sotak CH, Koretsky AP. Controlled aggregation of ferritin to modulate MRI relaxivity. *Biophys J* 2008, 95:342–351.
  196. Ichikawa T, Hogemann D, Saeki Y, Tyminski E, Terada K, Weissleder R, Chiocca EA, Basilion JP. MRI of transgene expression: correlation to therapeutic gene expression. *Neoplasia* 2002, 4:523–530.
  197. Wang K, Wang K, Shen B, Huang T, Sun X, Li W, Jin G, Li L, Bu L, Li R, et al. MR reporter gene imaging of endostatin expression and therapy. *Mol Imaging Biol* 2010, 12:520–529.
  198. Patrick PS, Hammersley J, Loizou L, Kettunen MI, Rodrigues TB, Hu D-E, Tee S-S, Hesketh R, Lyons SK, Soloviev D, et al. Dual-modality gene reporter for in vivo imaging. *Proc Natl Acad Sci USA* 2014, 111:415–420.
  199. Tannous BA, Grimm J, Perry KF, Chen JW, Weissleder R, Breakefield XO. Metabolic biotinylation of cell surface receptors for in vivo imaging. *Nat Methods* 2006, 3:391–396.
  200. Pereira S, Moss D, Williams S, Murray P, Taylor A. Overexpression of the MRI reporter genes ferritin and transferrin receptor affect iron homeostasis and produce limited contrast in mesenchymal stem cells. *Int J Mol Sci* 2015, 16:15481.
  201. Bernau K, Lewis CM, Petelinsek AM, Reagan MS, Niles DJ, Mattis VB, Meyerand ME, Suzuki M, Svendsen CN. In vivo tracking of human neural progenitor cells in the rat brain using magnetic resonance imaging is not enhanced by ferritin expression. *Cell Transplant* 2016, 25:575–592.
  202. Adams CW. Perivascular iron deposition and other vascular damage in multiple sclerosis. *J Neurol Neurosurg Psychiatry* 1988, 51:260–265.
  203. Rigol M, Solanes N, Roque M, Farre J, Batlle M, Roura S, Bellera N, Prat-Vidal C, Sionis A, Ramirez J, et al. Hemosiderin deposits confounds tracking of iron-oxide-labeled stem cells: an experimental study. *Transplant Proc* 2008, 40:3619–3622.
  204. Arosio P, Levi S. Cytosolic and mitochondrial ferritins in the regulation of cellular iron homeostasis and oxidative damage. *Biochim Biophys Acta* 1800, 2010:783–792.
  205. Loncar R, Flesche CW, Deussen A. Myocardial ferritin content is closely related to the degree of ischemia. *Acta Physiol Scand* 2004, 180:21–28.
  206. Robey TE, Murry CE. Absence of regeneration in the MRL/MpJ mouse heart following infarction or cryoinjury. *Cardiovasc Pathol* 2008, 17:6–13.
  207. Fischer UM, Harting MT, Jimenez F, Monzon-Posadas WO, Xue H, Savitz SI, Laine GA, Cox CS Jr. Pulmonary passage is a major obstacle for intravenous stem cell delivery: the pulmonary first-pass effect. *Stem Cells Dev* 2009, 18:683–692.
  208. Harting MT, Jimenez F, Xue H, Fischer UM, Baumgartner J, Dash PK, Cox CS. Intravenous mesenchymal stem cell therapy for traumatic brain injury: laboratory investigation. *J Neurosurg* 2009, 110:1189–1197.
  209. Everaert BR, Bergwerf I, De Vocht N, Ponsaerts P, Van Der Linden A, Timmermans J-P, Vrints CJ. Multimodal in vivo imaging reveals limited allograft survival, intrapulmonary cell trapping and minimal evidence for ischemia-directed BMSC homing. *BMC Biotechnol* 2012, 12:93.
  210. Urnov FDRE, Holmes MC, Zhang HS, Gregory PD. Genome editing with engineered zinc finger nucleases. *Nat Rev Genet* 2010, 11:636–646.
  211. Ochiai HSN, Fujita K, Nishikawa M, Suzuki K, Matsuura S, Miyamoto T, Sakuma T, Shibata T, Yamamoto T. Zinc-finger nuclease-mediated targeted insertion of reporter genes for quantitative imaging of gene expression in sea urchin embryos. *Proc Natl Acad Sci USA* 2012, 109:10915–10920.
  212. Wang YZW, Hu S, Lan F, Lee AS, Huber B, Lisowski L, Liang P, Huang M, de Almeida PE, Won JH, et al. Genome editing of human embryonic stem cells and induced pluripotent stem cells with zinc finger nucleases for cellular imaging. *Circ Res* 2012, 111:1494–1503.
  213. Yang HWH, Shivalila CS, Cheng AW, Shi L, Jaenisch R. One-step generation of mice carrying reporter and conditional alleles by CRISPR/Cas-mediated genome engineering. *Cell* 2013, 154:1370–1379.
  214. Horii T, Tamura D, Morita S, Kimura M, Hatada I. Generation of an ICF syndrome model by efficient genome editing of human induced pluripotent stem cells using the CRISPR system. *Int J Mol Sci* 2013, 14:19774–19781.
  215. Sommer DPA, Wirtz T, Mai M, Ackermann J, Thabet Y, Schmidt J, Weighardt H, Wunderlich FT, Degen J, Schultze JL, et al. Efficient genome engineering by targeted homologous recombination in mouse embryos using transcription activator-like effector nucleases. *Nat Commun* 2014, 5:3045.
  216. Kobayashi T, Kato-Itoh M, Yamaguchi T, Tamura C, Sanbo M, Hirabayashi M, Nakauchi H. Identification of rat Rosa26 locus enables generation of knock-in rat lines ubiquitously expressing tdTomato. *Stem Cells Dev* 2012, 21:2981–2986.

217. Cerbini T, Luo Y, Rao MS, Zou J. Transfection, selection, and colony-picking of human induced pluripotent stem cells TALEN-targeted with a GFP gene into the AAVS1 safe harbor. *J Vis Exp* 2015, 96:e52504.
218. Sadelain M, Papapetrou EP, Bushman FD. Safe harbours for the integration of new DNA in the human genome. *Nat Rev Cancer* 2012, 12:51–58.
219. Cozzi A, Corsi B, Levi S, Santambrogio P, Albertini A, Arosio P. Overexpression of wild type and mutated human ferritin H-chain in HeLa cells: in vivo role of ferritin ferroxidase activity. *J Biol Chem* 2000, 275:25122–25129.
220. Picard V, Renaudie F, Porcher C, Hentze MW, Grandchamp B, Beaumont C. Overexpression of the ferritin H subunit in cultured erythroid cells changes the intracellular iron distribution. *Blood* 1996, 87:2057–2064.
221. Kaur D, Rajagopalan S, Chinta S, Kumar J, Di Monte D, Cherny RA, Andersen JK. Chronic ferritin expression within murine dopaminergic midbrain neurons results in a progressive age-related neurodegeneration. *Brain Res* 2007, 1140:188–194.
222. Schuldiner M, Itskovitz-Eldor J, Benvenisty N. Selective ablation of human embryonic stem cells expressing a “suicide” gene. *Stem Cells* 2003, 21:257–265.
223. Qiao H, Surti S, Choi SR, Raju K, Zhang H, Ponde DE, Kung HF, Karp J, Zhou R. Death and proliferation time course of stem cells transplanted in the myocardium. *Mol Imaging Biol* 2009, 11:408–414.
224. Yarnykh VL, Tartaglione EV, Ioannou GN. Fast macromolecular proton fraction mapping of the human liver in vivo for quantitative assessment of hepatic fibrosis. *NMR Biomed* 2015, 28:1716–1725.